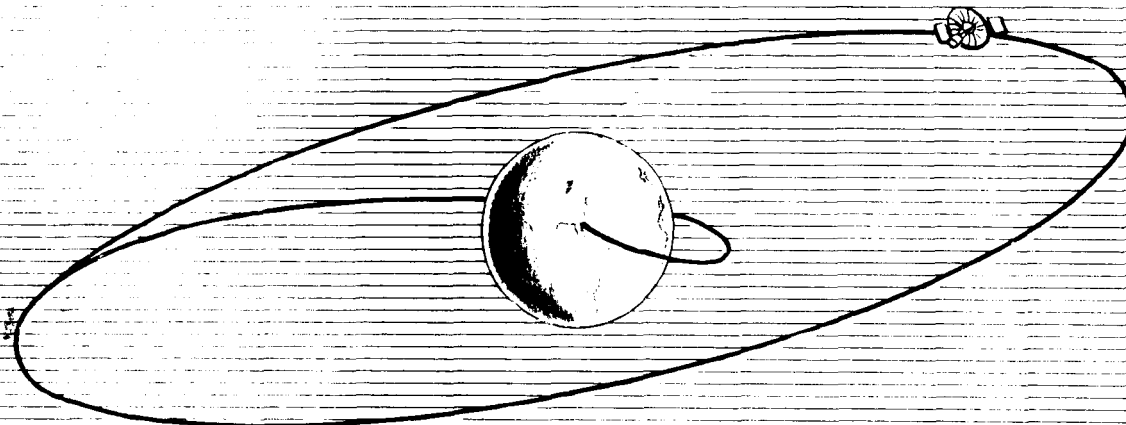


NASA-CR-81616



N67-24604

(ACCESSION NUMBER)

70

(PAGES)

CR-81616

(NASA CR OR TMX OR AD NUMBER)

(THRU)

1

(CODE)

31

(CATEGORY)

VOLUME 1 OF 8

# Final Report

## ATS - 4

PREPARED BY

**FAIRCHILD HILLER**  
SPACE SYSTEMS DIVISION

FOR

**NASA**  
**Goddard Space Flight Center**

DECEMBER 1966

ATS-4 STUDY PROGRAM

FINAL REPORT

(Contract NASW-1411)

VOLUME ONE OF EIGHT

prepared by

FAIRCHILD HILLER SPACE SYSTEMS DIVISION

Sherman Fairchild Technology Center

Germantown, Maryland

for

GODDARD SPACE FLIGHT CENTER

NATIONAL AERONAUTICS AND SPACE ADMINISTRATION

December 1966

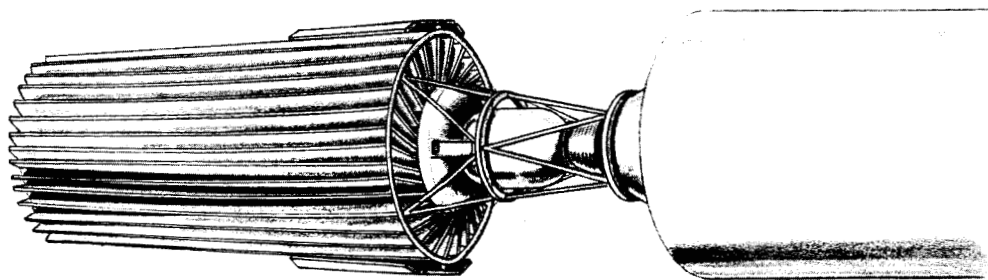
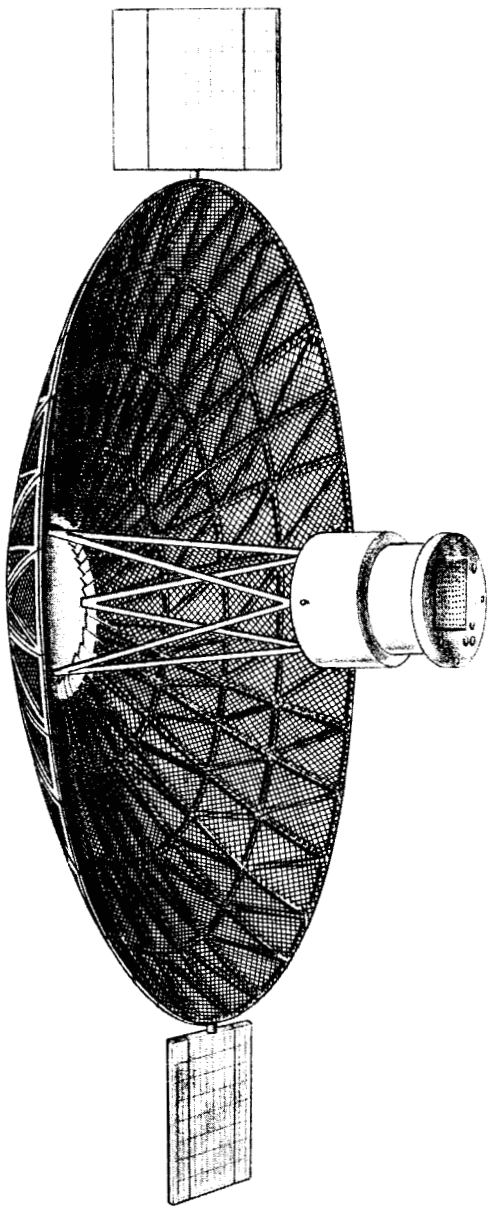


# TABLE OF CONTENTS

## VOLUME ONE

| Section | Title                                                       | Page |
|---------|-------------------------------------------------------------|------|
| 1.0     | Summary                                                     | 1-1  |
| 1.1     | Objectives and Justification                                | 1-1  |
|         | 1.1.1 Utilization                                           | 1-2  |
|         | 1.1.2 Implementation                                        | 1-4  |
| 1.2     | Program Feasibility                                         | 1-6  |
|         | 1.2.1 Parabolic Antenna                                     | 1-6  |
|         | 1.2.2 Stabilization and Control System                      | 1-8  |
|         | 1.2.3 Phased Array                                          | 1-11 |
|         | 1.2.4 Interferometer                                        | 1-12 |
| 1.3     | Subsystem Summaries                                         | 1-13 |
|         | 1.3.1 Configuration Description                             | 1-13 |
|         | 1.3.2 Parabolic Reflector                                   | 1-19 |
|         | 1.3.3 Parabolic Antenna Feed                                | 1-22 |
|         | 1.3.4 Attitude Stabilization and Control System             | 1-24 |
|         | 1.3.5 Launch Vehicle - Ascent and Orbit Injection           | 1-27 |
|         | 1.3.6 Interferometer System                                 | 1-32 |
|         | 1.3.7 Phased Array                                          | 1-33 |
|         | 1.3.8 In-Orbit Maneuvers and Auxiliary<br>Propulsion System | 1-35 |
|         | 1.3.9 Additional Experiment Capability                      | 1-37 |

# TABLE OF CONTENTS

## VOLUME TWO

| Section | Title                                      | Page  |
|---------|--------------------------------------------|-------|
| 2.0     | Systems Analysis                           | 2-1   |
| 2.1     | Mission Profile and Operations Plan        | 2-1   |
|         | 2.1.1 Mission Profile                      | 2-1   |
|         | 2.1.2 Operations Plan                      | 2-20  |
| 2.2     | Experiment Plan                            | 2-20  |
|         | 2.2.1 Parabolic Antenna Experiment         | 2-20  |
|         | 2.2.2 Monopulse System Operation           | 2-30  |
|         | 2.2.3 Phased Array Experiment              | 2-32  |
|         | 2.2.4 Orientation and Control Experiment   | 2-45  |
|         | 2.2.5 Interferometer Experiment            | 2-49  |
|         | 2.2.6 Additional Communication Experiments | 2-54  |
| 2.3     | Power Profiles                             | 2-58  |
|         | 2.3.1 Preorbital Power                     | 2-58  |
|         | 2.3.2 Experiment Evaluation                | 2-61  |
|         | 2.3.3 Experiment Demonstration             | 2-61  |
|         | 2.3.4 Power System Margin                  | 2-61  |
|         | 2.3.5 Experiment Loads                     | 2-64  |
| 2.4     | Antenna Accuracy Considerations            | 2-68  |
|         | 2.4.1 Reflecting Surface Errors            | 2-68  |
|         | 2.4.2 Feed Location Errors                 | 2-73  |
|         | 2.4.3 Frequency Limitations on Gain        | 2-74  |
|         | 2.4.4 Summary of Antenna Error Effects     | 2-76  |
| 2.5     | Antenna Efficiencies                       | 2-79  |
|         | 2.5.1 Parabolic Antenna                    | 2-79  |
|         | 2.5.2 Phased Array Figures of Merit        | 2-82  |
| 2.6     | Faisure Modes                              | 2-91  |
|         | 2.6.1 System Considerations                | 2-91  |
|         | 2.6.2 Parabolic Antenna                    | 2-91  |
|         | 2.6.3 Stabilization and Control System     | 2-93  |
|         | 2.6.4 Phased Array                         | 2-98  |
|         | 2.6.5 Antenna Experiment Electronics       | 2-100 |
|         | 2.6.6 Phased Array Monopulse Operation     | 2-103 |
| 2.7     | Weight Summaries                           | 2-105 |

# TABLE OF CONTENTS

## VOLUME THREE

| Section | Title                                            | Page  |
|---------|--------------------------------------------------|-------|
| 3.0     | Vehicle Engineering                              | 3-1   |
| 3.1     | Concept Evolution                                | 3-1   |
|         | 3.1.1 Trade-off Parameters                       | 3-1   |
|         | 3.1.2 F/D Trade-offs                             | 3-6   |
|         | 3.1.3 Spacecraft Concepts                        | 3-8   |
| 3.2     | Concept Evaluation and Reference Concept         | 3-21  |
|         | 3.2.1 Launch Vehicle Choice                      | 3-21  |
|         | 3.2.2 Split Module Concept                       | 3-21  |
|         | 3.2.3 Reference Concept                          | 3-25  |
|         | 3.2.4 Concept Comparison                         | 3-29  |
|         | 3.2.5 Titan IIIC Adaptability                    | 3-29  |
| 3.3     | Reflector Design                                 | 3-33  |
|         | 3.3.1 Design Evolution and Alternate Approaches  | 3-33  |
|         | 3.3.2 Petal Hinging Concepts                     | 3-38  |
|         | 3.3.3 Petal Structural Design                    | 3-40  |
|         | 3.3.4 Deployment System                          | 3-47  |
|         | 3.3.5 Tolerance Considerations                   | 3-47  |
|         | 3.3.6 Reflecting Surface                         | 3-50  |
|         | 3.3.7 Petal Locking System                       | 3-53  |
| 3.4     | Reflector Fabrication                            | 3-57  |
|         | 3.4.1 Fabrication Considerations                 | 3-57  |
|         | 3.4.2 Aluminum Substructure                      | 3-57  |
|         | 3.4.3 Wire Mesh Forming                          | 3-59  |
|         | 3.4.4 Sub-Assemblies                             | 3-60  |
|         | 3.4.5 Tooling                                    | 3-60  |
|         | 3.4.6 Assembly Procedure                         | 3-64  |
|         | 3.4.7 Measurement of Surface Deviations          | 3-65  |
| 3.5     | Structural and Dynamic Analyses                  | 3-71  |
|         | 3.5.1 Analytical Methods and Approach            | 3-71  |
|         | 3.5.2 Preliminary Analysis                       | 3-77  |
|         | 3.5.3 Integrated Spacecraft-Launch Configuration | 3-104 |
|         | 3.5.4 Integrated Spacecraft-Orbit Configuration  | 3-115 |
|         | 3.5.5 Orbit Maneuvering                          | 3-121 |

# TABLE OF CONTENTS

## VOLUME THREE (Continued)

| Section  | Title                                      | Page  |
|----------|--------------------------------------------|-------|
| 3.6      | Thermo/Structural Analysis                 | 3-129 |
|          | 3.6.1 Thermal Requirements and Approach    | 3-129 |
|          | 3.6.2 Design Orbit                         | 3-133 |
|          | 3.6.3 Petal Thermal Analysis               | 3-135 |
|          | 3.6.4 Thermoelastic Analysis of Reflector  | 3-154 |
|          | 3.6.5 Feed Mast Thermal Analysis           | 3-166 |
|          | 3.6.6 Thermal Deformation of Feed Mast     | 3-172 |
|          | 3.6.7 Spacecraft Thermal Control           | 3-175 |
| 3.7      | Dimensional Stability                      | 3-178 |
|          | 3.7.1 Introduction                         | 3-178 |
|          | 3.7.2 Precision Elastic Limit              | 3-179 |
|          | 3.7.3 Residual Stress                      | 3-179 |
|          | 3.7.4 Design Application                   | 3-180 |
|          | 3.7.5 References for Dimensional Stability | 3-182 |
|          | Discussion                                 |       |
| 3.8      | In-Orbit Measurement of Antenna Surface    | 3-183 |
|          | Accuracy                                   |       |
|          | 3.8.1 Basic Techniques                     | 3-183 |
|          | 3.8.2 Operational Considerations           | 3-183 |
|          | 3.8.3 Antenna Surface Errors               | 3-185 |
|          | 3.8.4 Equipment Location                   | 3-185 |
|          | 3.8.5 Conceptual Design                    | 3-186 |
|          | 3.8.6 Error Resolution Requirements        | 3-189 |
|          | 3.8.7 Sampling Surface Measurements        | 3-191 |
|          | 3.8.8 The Axial Four Camera System         | 3-192 |
|          | 3.8.9 Illumination of the Antenna          | 3-208 |
|          | 3.8.10 System Operation                    | 3-209 |
|          | 3.8.11 General Comments                    | 3-209 |
| Appendix |                                            |       |
| 3A       | Expandable Truss Antennas                  | 3-211 |
| 3B       | Inflatable Antennas                        | 3-225 |
| 3C       | Rigid Panel Antennas                       | 3-230 |
| 3D       | Petal Axis of Rotation Determination       | 3-248 |

# TABLE OF CONTENTS

## VOLUME FOUR

| Section | Title                                                  | Page |
|---------|--------------------------------------------------------|------|
| 4.0     | Power Systems                                          | 4-1  |
| 4.1     | Solar Panel Configuration Study                        | 4-2  |
| 4.2     | Solar Cell Radiation Degradation                       | 4-6  |
| 4.2.1   | Radiation Environment                                  | 4-6  |
| 4.2.2   | Background Flux                                        | 4-7  |
| 4.2.3   | Power Margin                                           | 4-10 |
| 4.3     | Battery Characteristics                                | 4-10 |
| 4.3.1   | Nickel-Cadmium Battery                                 | 4-13 |
| 4.3.2   | Silver-Cadmium Battery                                 | 4-13 |
| 4.3.3   | Silver-Zinc Battery                                    | 4-15 |
| 4.3.4   | Battery Comparison                                     | 4-15 |
| 4.4     | Battery Charging and Control                           | 4-23 |
| 4.4.1   | Constant Current Charging                              | 4-23 |
| 4.4.2   | Constant Voltage Charging                              | 4-24 |
| 4.4.3   | Modified Constant Voltage Charging                     | 4-26 |
| 4.4.4   | Tapered Charging                                       | 4-26 |
| 4.4.5   | Recommendation                                         | 4-26 |
| 4.5     | Concept Power Subsystem                                | 4-28 |
| 4.5.1   | Design Approach                                        | 4-28 |
| 4.5.2   | Battery Complement                                     | 4-32 |
| 4.5.3   | Solar Array                                            | 4-35 |
| 4.5.4   | Power Conditioning and Control                         | 4-36 |
| 5.0     | Orbital Analysis                                       | 5-1  |
| 5.1     | General                                                | 5-1  |
| 5.2     | Apogee Injection Stages                                | 5-2  |
| 5.3     | Ascent Trajectories                                    | 5-4  |
| 5.3.1   | Requirements and General Considerations                | 5-4  |
| 5.3.2   | Synchronous Injection - Single Apogee Impulse          | 5-7  |
| 5.3.3   | Subsynchronous Injection - High Altitude Parking Orbit | 5-10 |
| 5.3.4   | Recommended Centaur Ascent Trajectory                  | 5-18 |
| 5.4     | Orbit Payloads                                         | 5-23 |
| 5.4.1   | General                                                | 5-23 |
| 5.4.2   | SLV3A/Agna and SLV3C/Centaur                           | 5-23 |



TABLE OF CONTENTS  
VOLUME FOUR (Continued)

| Section | Title                                                     | Page |
|---------|-----------------------------------------------------------|------|
|         | 5.4.3 Titan IIIC                                          | 5-30 |
|         | 5.4.4 Payload Data Summary                                | 5-30 |
| 5.5     | Orbit Injection Errors                                    | 5-32 |
|         | 5.5.1 Error Values                                        | 5-32 |
|         | 5.5.2 Associated Latitude-Longitude Deviation             | 5-33 |
|         | 5.5.3 Associated Corrective Velocity Impulse Requirements | 5-36 |
| 5.6     | Orbit Perturbations                                       | 5-39 |
|         | 5.6.1 General                                             | 5-39 |
|         | 5.6.2 Earth Oblateness and Extraterrestrial Perturbations | 5-39 |
|         | 5.6.3 Terrestrial Perturbations - Equatorial Ellipticity  | 5-41 |
|         | 5.6.4 Associated Corrective Velocity Impulse Requirements | 5-45 |
| 5.7     | Auxiliary Propulsion System                               | 5-48 |
|         | 5.7.1 Velocity Impulse and Thrust Requirements            | 5-48 |
|         | 5.7.2 Initial APS Comparison Study                        | 5-48 |
| 5.8     | Orbit Guidance                                            | 5-57 |
|         | 5.8.1 General Requirements                                | 5-57 |
|         | 5.8.2 Orbit Injection Error Correction                    | 5-58 |
|         | 5.8.3 Station Keeping and Repositioning                   | 5-63 |
| 5.9     | References and Symbols for Orbital Analysis               | 5-65 |
|         | 5.9.1 References                                          | 5-65 |
|         | 5.9.2 List of Symbols                                     | 5-67 |

# TABLE OF CONTENTS

## VOLUME FIVE

| Section  | Title                                                                         | Page  |
|----------|-------------------------------------------------------------------------------|-------|
| 6.0      | ATTITUDE STABILIZATION AND CONTROL SYSTEM                                     | 6-1   |
| 6.1      | Attitude Stabilization and Control Requirements                               | 6-1   |
| 6.1.1    | Mission Requirements                                                          | 6-1   |
| 6.1.2    | Pointing Accuracy                                                             | 6-1   |
| 6.1.3    | Control Modes                                                                 | 6-1   |
| 6.2      | Attitude Reference Subsystem                                                  | 6-2   |
| 6.2.1    | Alternate Approaches                                                          | 6-2   |
| 6.2.2    | Candidate Reference Sensors                                                   | 6-11  |
| 6.2.3    | Selected Configuration                                                        | 6-22  |
| 6.2.4    | Sensor Performance                                                            | 6-23  |
| 6.3      | Disturbance Torque Model                                                      | 6-25  |
| 6.3.1    | Meteoroid Impact                                                              | 6-25  |
| 6.3.2    | Gravity Gradient                                                              | 6-34  |
| 6.3.3    | Magnetic Disturbance                                                          | 6-35  |
| 6.3.4    | Internal Rotating Equipment                                                   | 6-35  |
| 6.3.5    | Solar Pressure                                                                | 6-35  |
| 6.4      | Torquer Subsystem                                                             | 6-52  |
| 6.4.1    | Control Impulse Requirements                                                  | 6-52  |
| 6.4.2    | Candidate Reaction Jet Types                                                  | 6-59  |
| 6.4.3    | Inertia Wheel Subsystem                                                       | 6-63  |
| 6.4.4    | Selected Torquer Configuration                                                | 6-69  |
| 6.5      | Computation and Data Handling                                                 | 6-71  |
| 6.5.1    | On-Board Computation                                                          | 6-71  |
| 6.5.2    | Up-Data Commands                                                              | 6-71  |
| 6.5.3    | Down-Data Monitor                                                             | 6-71  |
| 6.6      | System Operational Description                                                | 6-75  |
| 6.6.1    | Control Mode Operation                                                        | 6-75  |
| 6.6.2    | System Block Diagram                                                          | 6-85  |
| 6.6.3    | Sensor Update                                                                 | 6-89  |
| 6.7      | System Performance                                                            | 6-90  |
| 6.7.1    | Pointing Accuracy                                                             | 6-90  |
| 6.7.2    | Acquisition                                                                   | 6-93  |
| 6.7.3    | Control System Dynamics                                                       | 6-93  |
| 6.7.4    | Reliability                                                                   | 6-117 |
| 6.8      | System Physical Description                                                   | 6-124 |
| Appendix |                                                                               |       |
| 6A       | Preliminary Control Torque and Impulse Requirements                           |       |
| 6B       | Preliminary Reaction Jet Considerations                                       |       |
| 6C       | Preliminary Inertia Wheel Considerations For Candidate Vehicle Configurations |       |
| 6D       | Preliminary Combined Wheel/Jet System Considerations                          |       |
| 6E       | Preliminary Transfer Orbit Control Mode Analysis                              |       |

# TABLE OF CONTENTS

## VOLUME SIX

| Section  | Title                                                     | Page  |
|----------|-----------------------------------------------------------|-------|
| 7.0      | Communications Experiments                                | 7-1   |
| 7.1      | Parabolic Antenna                                         | 7-1   |
|          | 7.1.1 Beam Scanning                                       | 7-1   |
|          | 7.1.2 Parabolic Antenna Feeds                             | 7-14  |
|          | 7.1.3 Aperture Blockage                                   | 7-32  |
|          | 7.1.4 Paraboloid Performance                              | 7-42  |
| 7.2      | Phased Array                                              | 7-58  |
|          | 7.2.1 Transdirective Array                                | 7-59  |
|          | 7.2.2 The Butler Matrix Array                             | 7-63  |
|          | 7.2.3 Space Fed (Lens) Array                              | 7-65  |
|          | 7.2.4 Corporate-Fed Array                                 | 7-71  |
|          | 7.2.5 Corporate-Fed Phased Array Design<br>Considerations | 7-79  |
|          | 7.2.6 Antenna Definition                                  | 7-92  |
|          | 7.2.7 Digital Beam Steering Unit                          | 7-102 |
|          | 7.2.8 Packaging Configuration                             | 7-108 |
| 7.3      | Communications Equipment                                  | 7-111 |
|          | 7.3.1 Transmission Parameters                             | 7-111 |
|          | 7.3.2 Systems Description                                 | 7-113 |
|          | 7.3.3 Weight, Volume and Power Summary                    | 7-134 |
|          | 7.3.4 System Performance Summary                          | 7-137 |
| Appendix |                                                           |       |
| 7A       | Four Paraboloid Off-Set Feed Configuration                | 7-139 |
| 7B       | Ionospheric Effects on Wave Polarization                  | 7-147 |
| 7C       | Separate 100 MHz Antennas                                 | 7-159 |
| 7D       | Communication Components                                  | 7-165 |

# TABLE OF CONTENTS

## VOLUME SEVEN

| Section  | Title                                                                                                                                           | Page  |
|----------|-------------------------------------------------------------------------------------------------------------------------------------------------|-------|
| 8.0      | Radio Interferometer Experiment                                                                                                                 | 8-1   |
| 8.1      | Introduction                                                                                                                                    | 8-1   |
| 8.2      | Study Approach                                                                                                                                  | 8-3   |
| 8.3      | Candidate Interferometer Concepts                                                                                                               | 8-5   |
| 8.4      | Candidate Interferometer Systems                                                                                                                | 8-11  |
|          | 8.4.1 Selection Criteria                                                                                                                        | 8-11  |
|          | 8.4.2 System Block Diagrams                                                                                                                     | 8-11  |
| 8.5      | Selection of Preferred Concept                                                                                                                  | 8-25  |
|          | 8.5.1 Candidate Evaluation and Selection of Preferred System                                                                                    | 8-25  |
|          | 8.5.2 Phased Array as an Interferometer                                                                                                         | 8-44  |
| 8.6      | Design of Preferred Interferometer System                                                                                                       | 8-48  |
|          | 8.6.1 General Circuit Description                                                                                                               | 8-48  |
|          | 8.6.2 Mechanical and Thermal Design                                                                                                             | 8-59  |
|          | 8.6.3 Interferometer Attitude Sensor Interface                                                                                                  | 8-68  |
|          | 8.6.4 Physical Characteristics                                                                                                                  | 8-85  |
| 8.7      | Error Analysis of Preferred Concept                                                                                                             | 8-86  |
| 8.8      | Conclusions and Recommendations                                                                                                                 | 8-116 |
| 8.9      | Bibliography and Glossary                                                                                                                       | 8-117 |
| Appendix |                                                                                                                                                 |       |
| 8A       | Interference Reduction by Correlation                                                                                                           | 8-136 |
| 8B       | RF Link Calculation                                                                                                                             | 8-138 |
| 8C       | Interferometer Angular Error Due to Mutual Coupling                                                                                             | 8-141 |
| 8D       | System Polarization                                                                                                                             | 8-146 |
| 8E       | Derivation of the Received Voltage Phases on an Elliptically Polarized Interferometer Antenna Pair with an Incident Elliptically Polarized Wave | 8-165 |
| 8F       | Alternative Antenna Switching Systems - Direct Phase Reading Interferometer                                                                     | 8-172 |
| 8G       | Derivation of Counter Equation                                                                                                                  | 8-180 |
| 8H       | Gating Time Error Analysis                                                                                                                      | 8-182 |
| 8I       | Conversion of $\theta_s$ into Attitude                                                                                                          | 8-187 |
| 8J       | Limitation of Range and Range Rate Capability                                                                                                   | 8-201 |
| Volume 8 | Program Budgetary Costs and Schedules                                                                                                           | 10-1  |

# TABLE OF CONTENTS

## VOLUME SEVEN (Continued)

| Section | Title                                                                      | Page  |
|---------|----------------------------------------------------------------------------|-------|
| 9.0     | Summary                                                                    | 9-1   |
| 9.1     | Data Flow                                                                  | 9-2   |
|         | 9.1.1 Definition                                                           | 9-2   |
|         | 9.1.2 Requirements                                                         | 9-2   |
|         | 9.1.3 Model of the Data Flow                                               | 9-3   |
| 9.2     | Telemetry System                                                           | 9-8   |
|         | 9.2.1 Data Handling Requirements                                           | 9-8   |
|         | 9.2.2 Data Handling System Design                                          | 9-9   |
|         | 9.2.3 Data Handling System Configuration                                   | 9-17  |
|         | 9.2.4 Data Transmission System Design                                      | 9-23  |
|         | 9.2.5 Data Transmission Link Calculation                                   | 9-28  |
|         | 9.2.6 System Size, Weight and Power Estimates                              | 9-44  |
|         | 9.2.7 Equipment Implementation                                             | 9-44  |
| 9.3     | Command System                                                             | 9-47  |
|         | 9.3.1 Definition                                                           | 9-47  |
|         | 9.3.2 Requirements                                                         | 9-47  |
|         | 9.3.3 Word Format                                                          | 9-50  |
|         | 9.3.4 Description and Operation of the Onboard System                      | 9-53  |
|         | 9.3.5 Estimates of Physical Characteristics                                | 9-60  |
|         | 9.3.6 Transmission Link Power Requirements                                 | 9-62  |
|         | 9.3.7 Equipment Implementation                                             | 9-64  |
|         | 9.3.8 Ground Equipment Requirements                                        | 9-65  |
| 9.4     | Range and Range Rate Transponder                                           | 9-69  |
|         | 9.4.1 Accuracy Requirements                                                | 9-69  |
|         | 9.4.2 Transponder Operating Frequency Selection                            | 9-69  |
|         | 9.4.3 UHF Transponder Characteristics                                      | 9-70  |
|         | 9.4.4 Equipment Implementation                                             | 9-71  |
| 9.5     | Ground Station Requirements                                                | 9-72  |
|         | 9.5.1 Ground Equipment Description                                         | 9-72  |
| 9.6     | References                                                                 | 9-84  |
|         | Appendices                                                                 |       |
|         | 9A Commutator Channel Assignment                                           | 9-85  |
|         | 9B Modulation Index Calculations (Mode 1)                                  | 9-101 |
|         | 9C Solving for Receiver Noise Power and Channel Bandwidth Ratios (Mode 1)  | 9-103 |
|         | 9D Solving for Receiver Noise Power and Channel Bandwidth Ratios (Mode II) | 9-105 |
|         | 9E Command Signal Catalog                                                  | 9-106 |
|         | 9F Telemetry Signal Catalog                                                | 9-116 |
|         | 9G Data Questionnaire                                                      | 9-131 |

# LIST OF ILLUSTRATIONS

## VOLUME ONE

| Figure | Title                          | Page |
|--------|--------------------------------|------|
| 1.3-1  | Fairchild Hiller ATS-4 Concept | 1-14 |
| 1.3-2  | Reference Concept              | 1-15 |
| 1.3-3  | Spacecraft Module Detail       | 1-18 |
| 1.3-4  | Multiband Prime Focus Feed     | 1-23 |
| 1.3-5  | SCS Block Diagram              | 1-29 |
| 1.3-6  | ATS-4 Ascent Trajectory        | 1-31 |

# LIST OF ILLUSTRATIONS

## VOLUME TWO

| Figure | Title                                                 | Page |
|--------|-------------------------------------------------------|------|
| 2.1-1  | Satellite Ground Track                                | 2-2  |
| 2.1-2  | Spacecraft/Sun Orientation in Transfer Orbit          | 2-4  |
| 2.1-3  | Satellite Ground Track and Ground Station             | 2-12 |
| 2.1-4  | Gross Data Flow Concept                               | 2-17 |
| 2.2-1  | Major Plane Location and Arts for Antenna Measurement | 2-22 |
| 2.2-2  | Ground Terminal Layout for Monopulse Calibration      | 2-33 |
| 2.2-3  | Major Planes and Beam Positions for Station Pattern   | 2-35 |
|        | Tests                                                 |      |
| 2.2-4  | Multiple Pattern Arts Using Two Ground Stations       | 2-41 |
| 2.2-5  | Crosstalk Measurement                                 | 2-41 |
| 2.2-6  | Major Plane Arts - Interferometer                     | 2-53 |
| 2.2-7  | Pointing of the Z-Axis for Interferometer Measurement | 2-53 |
| 2.3-1  | Typical Experiment Evaluation Profile                 | 2-62 |
| 2.3-2  | Power Profile with Additional Experiments             | 2-62 |
| 2.3-3  | Experiment Demonstration Maximum Profile              | 2-63 |
| 2.4-1  | Classification of Parabolic Antenna Errors            | 2-69 |
| 2.4-2  | Reflector Errors                                      | 2-71 |
| 2.4-3  | Feed Location Errors                                  | 2-75 |
| 2.4-4  | Feed Location Errors ( $F/D = 0.3$ )                  | 2-78 |
| 2.4-5  | Frequency Limitation on Gain                          | 2-78 |
| 2.5-1  | X-Band Radiation Pattern                              | 2-81 |
| 2.6-1  | Failed Reaction Wheel Backup Subsystem                | 2-94 |

# LIST OF ILLUSTRATIONS

## VOLUME THREE

| Figure | Title                                       | Page |
|--------|---------------------------------------------|------|
| 3.1-1  | Antenna Feed Location                       | 3-3  |
| 3.1-2  | C.G. Location Study                         | 3-5  |
| 3.1-3  | Concept SK513-10                            | 3-13 |
| 3.1-4  | Concept SK513-12                            | 3-15 |
| 3.1-5  | Concept SK513-11                            | 3-16 |
| 3.1-6  | Concept SK513-13                            | 3-17 |
| 3.1-7  | Concept SK513-14                            | 3-18 |
| 3.1-8  | Concept SK513-16                            | 3-19 |
| 3.2-1  | Concept SK513-18                            | 3-23 |
| 3.2-2  | Concept SK513-17 (Reference Concept)        | 3-24 |
| 3.2-3  | Spacecraft Module Detail                    | 3-27 |
| 3.2-4  | Concept Comparison Chart                    | 3-31 |
| 3.2-5  | Reference Concept on Titan IIC              | 3-32 |
| 3.3-1  | Conic Scissors Parabolic Antenna            | 3-34 |
| 3.3-2  | Inflatable Parabolic Antenna                | 3-36 |
| 3.3-3  | Retentive Memory Petal Concept              | 3-39 |
| 3.3-4  | Non-Radial Petals, Sheet One                | 3-41 |
| 3.3-5  | Non-Radial Petals, Sheet Two                | 3-42 |
| 3.3-6  | Petal Concept Parabolic Antenna             | 3-43 |
| 3.3-7  | Skewed Hinge Design                         | 3-45 |
| 3.3-8  | Petal Structural Assembly and Hinge Details | 3-46 |
| 3.3-9  | Deployment Synchronizer                     | 3-49 |
| 3.3-10 | Mesh Segment Installation                   | 3-51 |
| 3.3-11 | Mesh Reflector Characteristics              | 3-52 |
| 3.3-12 | Inter-Petal Locks                           | 3-55 |
| 3.3-13 | Inter-Petal Lock - Preferred Concept        | 3-56 |
| 3.4-1  | Shaping of Mesh Reflecting Surface          | 3-58 |
| 3.4-2  | Master Tool                                 | 3-58 |
| 3.4-3  | Assembly Bonding Fixture                    | 3-62 |
| 3.4-4  | Hinge and Latch Alignment Fixture           | 3-63 |
| 3.4-5  | Measurement of Surface Deviations           | 3-67 |
| 3.5-1  | Truss Feed Mast Weights                     | 3-78 |
| 3.5-2  | Truss Feed Mast Frequencies                 | 3-79 |
| 3.5-3  | Single Tube Feed Mast Analysis              | 3-81 |
| 3.5-4  | Four Tube Feed Mast Weights                 | 3-82 |
| 3.5-5  | Four Tube Feed Mast Frequencies             | 3-83 |
| 3.5-6  | Analysis of Quadruped Feed Mast Structure   | 3-84 |



LIST OF ILLUSTRATIONS  
VOLUME THREE (Continued)

| Figure | Title                                                                  | Page  |
|--------|------------------------------------------------------------------------|-------|
| 3.5-7  | Quadruped Feed Mast Frequencies                                        | 3-85  |
| 3.5-8  | Analysis of Tripod Feed Mast Structure                                 | 3-86  |
| 3.5-9  | Tripod Feed Mast Frequencies                                           | 3-87  |
| 3.5-10 | Reflector Petal Loading                                                | 3-94  |
| 3.5-11 | Spacecraft, Injection, Motor and Adapter<br>Structural Properties      | 3-94  |
| 3.5-12 | Launch Integrated S/C - Analytical Model                               | 3-96  |
| 3.5-13 | Orbit Configuration - Mass Model                                       | 3-102 |
| 3.5-14 | Preferred Configuration and Analytical Model                           | 3-105 |
| 3.5-15 | Petal Restraint and Stiffness                                          | 3-106 |
| 3.5-16 | Mass Point Locations and Weights                                       | 3-107 |
| 3.5-17 | YY Direction Mode Shapes                                               | 3-109 |
| 3.5-18 | XX Direction Mode Shapes                                               | 3-110 |
| 3.5-19 | Analytical Model - Orbit Configuration                                 | 3-116 |
| 3.5-20 | Frequency and Mode Shapes - Orbit Configuration,<br>Sheet One          | 3-118 |
| 3.5-21 | Frequency and Mode Shapes - Orbit Configuration,<br>Sheet Two          | 3-119 |
| 3.5-22 | Frequency and Mode Shapes - Orbit Configuration,<br>Sheet Three        | 3-120 |
| 3.5-23 | Response to Single Finite Duration Pulse<br>(Roll Correction Maneuver) | 3-124 |
| 3.5-24 | Response to Single Finite Duration Pulse<br>(Yaw Correction Maneuver)  | 3-125 |
| 3.6-1  | Yearly Change in Orbit Position Relative to<br>Sun Vector              | 3-134 |
| 3.6-2  | Petal Thermal Analysis                                                 | 3-136 |
| 3.6-3  | Relation of Thermal Analysis Nodes to Orbit Position                   | 3-136 |
| 3.6-4  | Feed Module Shadowing                                                  | 3-137 |
| 3.6-5  | Reflection Mesh Sunlight Blockage                                      | 3-139 |
| 3.6-6  | Mesh and Antenna Hub Shadowing                                         | 3-141 |
| 3.6-7  | Coordinate System for Thermal Analysis                                 | 3-142 |
| 3.6-8  | Antenna Feed Shadowing                                                 | 3-144 |
| 3.6-9  | Beam Temperatures                                                      | 3-147 |
| 3.6-10 | Petal Beam Cross-Section                                               | 3-151 |
| 3.6-11 | Mesh Standoff Fittings                                                 | 3-151 |

LIST OF ILLUSTRATIONS

VOLUME THREE (Continued)

| Figure | Title                                                           | Page   |
|--------|-----------------------------------------------------------------|--------|
| 3.6-12 | Beam Geometry                                                   | 3-153  |
| 3.6-13 | Petal Thermal Model                                             | 3-159  |
| 3.6-14 | Radial Displacement Geometry                                    | 3-159  |
| 3.6-15 | Deformation of Radial Member                                    | 3-159  |
| 3.6-16 | Reflector Surface Mesh Geometry                                 | 3-165  |
| 3.6-17 | Surface Mesh Chord Position                                     | 3-165  |
| 3.6-18 | Feed Mast Geometry                                              | 3-167  |
| 3.6-19 | Electrical Simulation, Uninsulated Mast                         | 3-168  |
| 3.6-20 | Electrical Simulation, Insulated Mast                           | 3-168a |
| 3.6-21 | Temperature of Node 4, Uninsulated Mast                         | 3-170  |
| 3.6-22 | Temperature of Node 4, Insulated Mast                           | 3-170a |
| 3.6-23 | Feed Mast Shadowing on Support "A"                              | 3-171  |
| 3.6-24 | Feed Mast Thermal Model                                         | 3-171a |
| 3.6-25 | Feed Mast Distortions                                           | 3-174  |
| 3.6-26 | Passive Control Areas Average Temperature<br>versus Dissipation | 3-176  |
| 3.8-1  | Volume Available for Measurement Equipment                      | 3-187  |
| 3.8-2  | Mirror Position above Camera                                    | 3-187  |
| 3.8-3  | Converse Mirror below Camera                                    | 3-187  |
| 3.8-4  | Concave Mirror below Camera                                     | 3-188  |
| 3.8-5  | Sighting Angles                                                 | 3-188  |
| 3.8-6  | Effective Mesh Spacing                                          | 3-188  |
| 3.8-7  | Composite Converse Mirror                                       | 3-192  |
| 3.8-8  | Basic Four Camera Axial System                                  | 3-192  |
| 3.8-9  | Full View Camera System                                         | 3-194  |
| 3.8-10 | Normal Deflection Geometry                                      | 3-194  |
| 3.8-11 | Ring Viewing Angles                                             | 3-194  |
| 3.8-12 | Vidicon Image Dimensions                                        | 3-196  |
| 3.8-13 | Central Circle in Vidicon Image                                 | 3-196  |
| 3.8-14 | Radial and Circular Scan Patterns                               | 3-198  |
| 3.8-15 | Rim Marker Pattern                                              | 3-198  |
| 3.8-16 | Modified Marker Coding                                          | 3-198  |
| 3.8-17 | Reversed Marker Pattern                                         | 3-201  |
| 3.8-18 | Marker Pattern without 1/2 Inch Plates                          | 3-201  |
| 3.8-19 | Pattern for Third Ring                                          | 3-202  |
| 3.8-20 | Pattern for Second Ring                                         | 3-202  |

LIST OF ILLUSTRATIONS

VOLUME THREE (Continued)

| Figure | Title                                                      | Page  |
|--------|------------------------------------------------------------|-------|
| 3.8-21 | Pattern for Central Ring                                   | 3-202 |
| 3.8-22 | Pattern of Perfect Match of Image and Standard<br>Negative | 3-203 |
| 3.8-23 | Pattern of Mismatch of Image and Standard Negative         | 3-203 |
| 3.8-24 | Marking Pattern from Deformed Mesh Wires                   | 3-207 |
| 3.8-25 | Deformed Wires Positioned along a Parabola                 | 3-207 |
| 3.8-26 | Illumination by Columnar Light Sources                     | 3-208 |
| 3.8-27 | Illumination by Toroidal Light Sources                     | 3-208 |

# LIST OF ILLUSTRATIONS

## VOLUME FOUR

| Figure | Title                                                                 | Page |
|--------|-----------------------------------------------------------------------|------|
| 4.1-1  | Flat Plate Array, Two Degrees Of Freedom                              | 4-3  |
| 4.1-2  | Flat Plate Array, One Degree Of Freedom                               | 4-3  |
| 4.1-3  | Flat Plate Array, Fixed                                               | 4-3  |
| 4.1-4  | Two Flat Plates Array, Fixed                                          | 4-4  |
| 4.1-5  | Three Flat Plates Array, Fixed                                        | 4-4  |
| 4.1-6  | Cylindrical Array, Fixed                                              | 4-4  |
| 4.1-7  | Double Faced Flat Plate Array                                         | 4-5  |
| 4.1-8  | Double Faced Two Flat Plates Array                                    | 4-5  |
| 4.1-9  | Double Faced Three Flat Plates Array                                  | 4-5  |
| 4.2-1  | Solar Cell Radiation Degradation                                      | 4-8  |
| 4.2-2  | Power Loss Due To Radiation Effects                                   | 4-11 |
| 4.3-1  | Nickel-Cadmium Battery Life                                           | 4-14 |
| 4.3-2  | Energy Per Unit Weight For Various Batteries                          | 4-17 |
| 4.3-3  | Energy Per Unit Volume For Various Batteries                          | 4-18 |
| 4.3-4  | Capacity vs. Temperature For Various Cells                            | 4-18 |
| 4.3-5  | Silver-Zinc Battery Cycle Life                                        | 4-19 |
| 4.3-6  | Silver-Cadmium Battery Cycle Life                                     | 4-19 |
| 4.3-7  | Nickel-Cadmium Battery Cycle Life                                     | 4-20 |
| 4.3-8  | Umbra and Penumbra Patterns For A<br>Synchronous Equatorial Satellite | 4-22 |
| 4.4-1  | Recommended % Overcharge is Temperature                               | 4-25 |
| 4.4-2  | Overcharge Pressure Vs Current                                        | 4-25 |
| 4.4-3  | Maximum Limiting Voltage Vs. Temperature                              | 4-27 |
| 4.4-4  | Tapered Charge Characteristic                                         | 4-27 |
| 4.5-1  | Typical Experiment Evaluation Power Profile                           | 4-29 |
| 4.5-2  | Power Profile With Additional Experiments                             | 4-29 |
| 4.5-3  | Experiment Demonstration Maximum Demand<br>Profile                    | 4-29 |
| 4.5-4  | Power System Weight Vs. Load Duration                                 | 4-29 |
| 4.5-5  | Power System Block Diagram                                            | 4-37 |

# LIST OF ILLUSTRATIONS

## VOLUME FOUR (Continued)

| Figure | Title                                                                    | Page |
|--------|--------------------------------------------------------------------------|------|
| 5.3-1  | Ascent Trajectories                                                      | 5-6  |
| 5.3-2  | Earth Track of Ascent Trajectory                                         | 5-11 |
| 5.3-3  | Injection Station Longitude Variation                                    | 5-11 |
| 5.3-4  | Effect of Launch Azimuth on Required Increase in Characteristic Velocity | 5-14 |
| 5.3-5  | High Altitude, Elliptic Parking Orbit Characteristics                    | 5-16 |
| 5.3-6  | Earth Track of High Altitude Parking Orbit Ascent Trajectory             | 5-17 |
| 5.3-7  | Ground Track of Ascent Trajectories                                      | 5-19 |
| 5.3-8  | Spacecraft/Sun Orientation in Transfer Orbit                             | 5-21 |
| 5.4-1  | Payload and AIS Propellant Weight vs $i_c$ (Burner II)                   | 5-28 |
| 5.4-2  | Payload and AIS Propellant Weight vs $i_c$ (TE364-3)                     | 5-28 |
| 5.6-1  | Satellite Semimajor Axis Perturbation                                    | 5-42 |
| 5.6-2  | Satellite Inclination Perturbation                                       | 5-42 |
| 5.6-3  | Long Period Oscillation                                                  | 5-44 |
| 5.6-4  | Required Velocity Impulse per Year                                       | 5-46 |

# LIST OF ILLUSTRATIONS

## VOLUME FIVE

| Figure | Title                                                                           | Page  |
|--------|---------------------------------------------------------------------------------|-------|
| 6-1    | Reference Coordinate Frame (Nominal)                                            | 6-3   |
| 6-2a   | Cell Orientation                                                                | 6-13  |
| 6-2b   | Cell Outputs                                                                    | 6-13  |
| 6-2c   | Sun Sensor Signals                                                              | 6-13  |
| 6-3    | Meteoroid Extrapolations                                                        | 6-29  |
| 6-4    | Percent Open Area in Each Mesh Segment as a<br>Function of Solar Incident Angle | 6-41  |
| 6-5    | Antenna Projected Surface Map                                                   | 6-43  |
| 6-6    | Projected Antenna Shaded Area Profile                                           | 6-44  |
| 6-7    | Pitch Axis Solar Pressure Disturbance Torque                                    | 6-47  |
| 6-8    | Roll Axis Solar Pressure Disturbance Torque Due<br>to Antenna and Feed System   | 6-48  |
| 6-9    | Roll Axis Solar Pressure Disturbance Torque Due<br>to Fixed Solar Panels Only   | 6-49  |
| 6-10   | Roll Axis Solar Pressure Disturbance Torque                                     | 6-50  |
| 6-11   | Yaw Axis Solar Pressure Disturbance Torque                                      | 6-51  |
| 6-12   | Hydrazine Thruster Output Efficiency                                            | 6-62  |
| 6-13   | Liquid Hydrazine System Schematic                                               | 6-64  |
| 6-14   | Block Diagram - Ascent Control                                                  | 6-86  |
| 6-15   | SCS Block Diagram                                                               | 6-87  |
| 6-16   | Phase Plane Plot Sun Acquisition - Pitch Axis                                   | 6-94  |
| 6-17   | Phase Plane Plot Sun Acquisition - Yaw Axis                                     | 6-95  |
| 6-18   | Phase Plane Plot Earth Acquisition Roll Axis                                    | 6-96  |
| 6-19   | Phase Plane Plot Star Acquisition Yaw Axis                                      | 6-97  |
| 6-20   | Open Loop Bode Plot - Roll Axis                                                 | 6-99  |
| 6-21   | Open Loop Bode Plot - Pitch Axis                                                | 6-100 |
| 6-22   | Open Loop Bode Plot - Yaw Axis                                                  | 6-101 |
| 6-23   | SCS and Vehicle Dynamics Block Diagram                                          | 6-102 |
| 6-24   | Roll Axis - Rigid Body Amplitude Response                                       | 6-104 |
| 6-25   | Roll Axis - Rigid Body Phase Response                                           | 6-105 |
| 6-26   | Pitch Axis - Rigid Body Amplitude Response                                      | 6-106 |
| 6-27   | Pitch Axis - Rigid Body Phase Response                                          | 6-107 |
| 6-28   | Amplitude Response Roll Axis - Flexible (.01)                                   | 6-108 |
| 6-29   | Phase Response Roll Axis - Flexible (.01)                                       | 6-109 |
| 6-30   | Phase Response Pitch Axis - Flexible (.01)                                      | 6-110 |
| 6-31   | Phase Response Pitch Axis - Flexible (.01)                                      | 6-111 |
| 6-32   | Amplitude Response Roll Axis - Flexible (.005)                                  | 6-112 |
| 6-33   | Phase Response Roll Axis - Flexible (.005)                                      | 6-113 |
| 6-34   | Amplitude Response Pitch Axis - Flexible (.005)                                 | 6-114 |

# LIST OF ILLUSTRATIONS

## VOLUME FIVE (Continued)

| Figure | Title                                                           | Page  |
|--------|-----------------------------------------------------------------|-------|
| 6-35   | Phase Response Pitch Axis - Flexible (.005)                     | 6-115 |
| 6-36   | Phase Plane Plot Attitude Control During Station Keeping        | 6-118 |
| 6-37   | Reliability Diagram                                             | 6-119 |
| 6A-1   | Limit Cycle Impulse Requirements                                | 6A-7  |
| 6A-2   | Disturbance Torque Impulse Requirements                         | 6A-8  |
| 6A-3   | Maneuver Impulse Requirements                                   | 6A-9  |
| 6B-1   | Micro-Rocket Applicability Thrust and Total Impulse             | 6B-4  |
| 6B-2   | Micro-Rocket Applicability Thrust and Duty Cycle                | 6B-5  |
| 6B-3   | Estimated System Weight as a Function of On Board Total Impulse | 6B-7  |
| 6B-4   | Reliability Comparison of Bipropellant or Monopropellant System | 6B-8  |
| 6B-5   | Hydrazine Plenum System Schematic                               | 6B-10 |
| 6B-6   | Liquid Hydrazine System Schematic                               | 6B-11 |

# LIST OF ILLUSTRATIONS

## VOLUME SIX

| Figure | Title                                                                         | Page |
|--------|-------------------------------------------------------------------------------|------|
| 7.1-1  | Prime Focus Paraboloid Scanning Performance                                   | 7-3  |
| 7.1-2  | Paraboloid Gain Loss as a Function of Beamwidths Scanned                      | 7-4  |
| 7.1-3  | Beam Scanning Capability of a Multi-Element Paraboloid Switching -Feed System | 7-7  |
| 7.1-4  | Beam Cross-Over Level as a Function of the Beam Scanning Increment            | 7-8  |
| 7.1-5  | Cassegrain Antenna Gain Loss with Subdish Rotation                            | 7-11 |
| 7.1-6  | Radiation Characteristics of a Tapered Circular Aperture                      | 7-16 |
| 7.1-7  | Paraboloid Subtended Angle and Feed Size as a Function of the F/D Ratio       | 7-18 |
| 7.1-8  | S-Band Feed-Edge Taper                                                        | 7-23 |
| 7.1-9  | 800 MHz Prime Focus Feed                                                      | 7-24 |
| 7.1-10 | 100 MHz Prime Focus Feed                                                      | 7-27 |
| 7.1-11 | Spiral Antenna Monopulse Operation                                            | 7-29 |
| 7.1-12 | Parabolic Antenna Gain Loss as a Function of the Blockage Ratio               | 7-34 |
| 7.1-13 | X-Band Radiation Pattern                                                      | 7-35 |
| 7.1-14 | Antenna Test Range                                                            | 7-38 |
| 7.1-15 | Source Tower                                                                  | 7-39 |
| 7.1-16 | Feed Support Mast                                                             | 7-44 |
| 7.1-17 | Paraboloid Assembly                                                           | 7-45 |
| 7.1-18 | Back View of Feed Support                                                     | 7-46 |
| 7.1-19 | Left Side View of Feed and Feed Support                                       | 7-47 |
| 7.1-20 | Right Side View of Feed and Feed Support                                      | 7-48 |
| 2.1-21 | Right Side View of Feed                                                       | 7-49 |
| 7.1-22 | Feeds, End View                                                               | 7-50 |
| 7.1-23 | Feeds, Side View                                                              | 7-51 |
| 7.1-24 | E-Plane Radiation Patterns, Frequency 4.6 GHz                                 | 7-52 |
| 7.1-25 | E-Plane Radiation Patterns, Frequency 10.5 GHz                                | 7-53 |
| 7.1-26 | E-Plane Radiation Patterns, Frequency 12.0 GHz                                | 7-54 |
| 7.1-27 | E-Plane Radiation Pattern, Frequency 18.0 GHz                                 | 7-55 |
| 7.1-28 | E-Plane Radiation Pattern, Frequency 29.6 GHz                                 | 7-56 |



# LIST OF ILLUSTRATIONS

## VOLUME SIX (Continued)

| Figure | Title                                                                                       | Page  |
|--------|---------------------------------------------------------------------------------------------|-------|
| 7.2-1  | Transdirective Array                                                                        | 7-60  |
| 7.2-2  | Butler Matrix Array - Block Diagram                                                         | 7-64  |
| 7.2-3  | Space Fed (Lens) Array - Block Diagram                                                      | 7-67  |
| 7.2-4  | Stripline Diplexer                                                                          | 7-69  |
| 7.2-5  | Stripline Latching Phase Shifter                                                            | 7-70  |
| 7.2-6  | Corporate-Fed Array                                                                         | 7-72  |
| 7.2-7  | Artist Conception of Corporate-Fed Array                                                    | 7-75  |
| 7.2-8  | Schematic of Microwave Subsystem                                                            | 7-80  |
| 7.2-9  | Detail of Feed Horn Assembly                                                                | 7-83  |
| 7.2-10 | Possible Configuration of 4 Channel Diplexer -<br>Circulator Strip Line Module              | 7-86  |
| 7.2-11 | Waveguide Latching Phase Shifter                                                            | 7-89  |
| 7.2-12 | Array Element Layout                                                                        | 7-94  |
| 7.2-13 | Phased Array Patterns                                                                       | 7-95  |
| 7.2-14 | Phased Array Beam Spacing                                                                   | 7-101 |
| 7.2-15 | Block Diagram for Digital Beam Steering Unit                                                | 7-103 |
| 7.2-16 | Schematic Diagram for Bit Driver                                                            | 7-105 |
| 7.2-17 | Plan View of Radiating Elements                                                             | 7-107 |
| 7.2-18 | Side View of Corporate-Fed Array                                                            | 7-108 |
| 7.2-19 | End View of Corporate-Fed Array                                                             | 7-109 |
| 7.3-1  | RF Power vs Ground Antenna Gain                                                             | 7-116 |
| 7.3-2  | ATS-4 Communications System                                                                 | 7-119 |
| 7.3-3  | Frequency Generator                                                                         | 7-120 |
| 7.3-4  | Monopulse and Phased Array X-Band Transfer<br>Characteristics-Series 100                    | 7-126 |
| 7.3-5  | 100 MHz Relay Transfer Characteristics-Series 200                                           | 7-127 |
| 7.3-6  | X-Band Transponder Output-Reflector and Phased<br>Array Transfer Characteristics-Series 300 | 7-128 |
| 7.3-7  | 800 MHz Relay Transfer Characteristics-Series 400                                           | 7-129 |
| 7.3-8  | Filter Response                                                                             | 7-130 |
| 7.3-9  | S-Band Data Link Transfer Characteristics-<br>Series 500                                    | 7-131 |
| 7.3-10 | X-Band Frequency Generator-Representative<br>Transfer Characteristics-Series 600            | 7-132 |
| 7.3-11 | Multipliers in Frequency Generator, Represen-<br>tative Transfer Characteristics-Series 700 | 7-135 |

# LIST OF ILLUSTRATIONS

## VOLUME SLX (Continued)

| Figure | Title                                                                                             | Page  |
|--------|---------------------------------------------------------------------------------------------------|-------|
| 7A-1   | Four Paraboloid Offset Feed Configuration                                                         | 7-140 |
| 7A-2   | Radiation Pattern of a 15-Foot Paraboloid 10 db<br>Tapered Distribution                           | 7-141 |
| 7A-3   | Radiation Pattern Four Paraboloid Array                                                           | 7-142 |
| 7A-4   | Monopulse Radiation Pattern of the Four Paraboloid<br>Array                                       | 7-144 |
| 7A-5   | Four Paraboloid Array Scanning Performance                                                        | 7-145 |
| 7B-1   | Faraday Rotation as a Function of Frequency                                                       | 7-152 |
| 7B-2   | Attenuation between Arbitrarily Polarized Antenna<br>Caused by Faraday Rotation AF - Axial Ratio  | 7-156 |
| 7B-3   | Attenuation between Arbitrarily Polarized Antennas<br>Caused by Faraday Rotation AR - Axial Ratio | 7-158 |
| 7C-1   | Helical Antenna Gain as a Function of Antenna<br>Length                                           | 7-161 |
| 7C-2   | Array Element Spacing as a Function of Array<br>Element Gain                                      | 7-163 |

# LIST OF ILLUSTRATIONS

## VOLUME SEVEN

| Figure | Title                                                                                                                       | Page |
|--------|-----------------------------------------------------------------------------------------------------------------------------|------|
| 8.4-1  | LF Phase Reading Interferometer                                                                                             | 8-13 |
| 8.4-2  | RMS Phase Difference Reading Interferometer<br>Technique                                                                    | 8-16 |
| 8.4-3  | RF Cross Correlation Interferometer Technique                                                                               | 8-19 |
| 8.4-4  | Spread Spectrum Interferometer Technique                                                                                    | 8-22 |
| 8.5-1  | Resultant Nonambiguous Pattern after Correlation                                                                            | 8-26 |
| 8.5-2  | Partial System Schematic of Cross Correlator<br>Interferometer                                                              | 8-30 |
| 8.5-3  | Monopulse Space Angle RMS Error                                                                                             | 8-31 |
| 8.5-4  | RMS Space Angle Error Direct Phase Reading<br>Interferometer                                                                | 8-33 |
| 8.5-5  | Direct Phase Reading Interferometer Relationship,<br>Space Angle Element Separation, Unambiguous<br>Interval vs $D/\lambda$ | 8-36 |
| 8.5-6  | Interferometer Phase Error Due to Temperature<br>Differential in Transmission Lines                                         | 8-37 |
| 8.5-7  | Layout of Phased Array                                                                                                      | 8-45 |
| 8.6-1  | Direct Phase Reading Interferometer                                                                                         | 8-48 |
| 8.6-2  | Interferometer                                                                                                              | 8-53 |
| 8.6-3  | Horn Design                                                                                                                 | 8-63 |
| 8.6-4  | Interferometer Thermal Flow Diagrams                                                                                        | 8-66 |
| 8.6-5  | Interface between the SCS and Interferometer                                                                                | 8-69 |
| 8.6-6  | Mode Selection and Phase Measurement                                                                                        | 8-72 |
| 8.6-7  | Timing Diagram for Phase Measurement                                                                                        | 8-74 |
| 8.6-8  | Arithmetic Unit for $\epsilon'_z + \epsilon''_z$ and $\epsilon'_y + \epsilon''_y$                                           | 8-78 |
| 8.6-9  | Arithmetic Unit for $\epsilon'_x + \epsilon''_x$                                                                            | 8-79 |
| 8.6-10 | Timing Diagram for Computational Instruction                                                                                | 8-81 |
| 8.6-11 | Time Distribution of the Arithmetic Units                                                                                   | 8-82 |
| 8.7-1  | System Model                                                                                                                | 8-87 |
| 8.7-2  | Simplified Block Diagram of Direct Phase Reading<br>Electronics                                                             | 8-88 |
| 8.7-3  | Basic Interferometer Relationship                                                                                           | 8-90 |
| 8.7-4  | Geometrical Relationship of Spacecraft Position and<br>Ground Station                                                       | 8-92 |
| 8.7-5  | Error in Count vs $\theta_s$                                                                                                | 8-96 |
| 8.7-6  | Refraction Effects                                                                                                          | 8-97 |
| 8.7-7  | Atmospheric Effect on Elevation Angle                                                                                       | 8-98 |
| 8.7-8  | Atmospheric Effect on the Slant Range Difference                                                                            | 8-99 |

# LIST OF ILLUSTRATIONS

## VOLUME SEVEN (Continued)

| Figure | Title                                                                                                             | Page  |
|--------|-------------------------------------------------------------------------------------------------------------------|-------|
| 8.7-9  | Spacecraft Coordinate System                                                                                      | 8-105 |
| 8.7-10 | Pitch Axis $3\sigma$ Error vs Pitch Angle, $\theta$                                                               | 8-107 |
| 8.7-11 | Yaw Axis $3\sigma$ Error vs Pitch Angle, $\theta$                                                                 | 8-108 |
| 8.7-12 | Vector Diagram of Satellite - Ground Station Geometry                                                             | 8-109 |
| 8.7-13 | Orientation of $R_s$                                                                                              | 8-113 |
| 8B-1   | ERP vs SNR                                                                                                        | 8-140 |
| 8C-1   | Space Angular Error ( $\Delta\theta_m$ ) vs Antenna Separation ( $D/\lambda$ ) for Different Mutual Couplings (C) | 8-142 |
| 8C-2   | Space Angle Error Due to Mutual Coupling - Coarse Antenna Pair                                                    | 8-143 |
| 8C-3   | Comparison of Antenna Elements - Mutual Coupling                                                                  | 8-145 |
| 8D-1   | Elliptically Polarized Interferometer Antenna Pair with Elliptically Polarized Incoming Wave                      | 8-149 |
| 8D-2   | Phase Angle Error vs Axial Ratio Inequality                                                                       | 8-152 |
| 8D-3   | Phase Angle Error vs Ellipse Tilt Angle Inequality                                                                | 8-155 |
| 8D-4   | Phase Angle Error vs Roll Angle ( $\delta$ )                                                                      | 8-160 |
| 8D-5   | Phase Angle Error vs Pitch Angle ( $\theta$ )                                                                     | 8-161 |
| 8E-1   | Elliptically Polarized Plane Wave                                                                                 | 8-166 |
| 8E-2   | Elliptically Polarized Plane Wave Incident at Angles $\theta$ , $\delta$                                          | 8-167 |
| 8E-3   | Receive Antenna with Inclined Polarization Ellipse                                                                | 8-168 |
| 8F-1   | Switched Signal Lines                                                                                             | 8-174 |
| 8F-2   | Switched Oscillator Lines                                                                                         | 8-175 |
| 8F-3   | Switched IF Lines                                                                                                 | 8-176 |
| 8F-4   | Switched Multipliers                                                                                              | 8-177 |
| 8H-1   | Phase Error Distribution at Start of Count                                                                        | 8-186 |
| 8H-2   | Phase Error Distribution at End of Count                                                                          | 8-186 |
| 8H-3   | Phase Error Density Function                                                                                      | 8-186 |
| 8I-1   | Interferometer Illumination                                                                                       | 8-188 |
| 8I-2   | Satellite Orientation                                                                                             | 8-193 |
| 8J-1   | Geometry for Range and Range Rate Analysis                                                                        | 8-201 |

# LIST OF ILLUSTRATIONS

## VOLUME SEVEN (Continued)

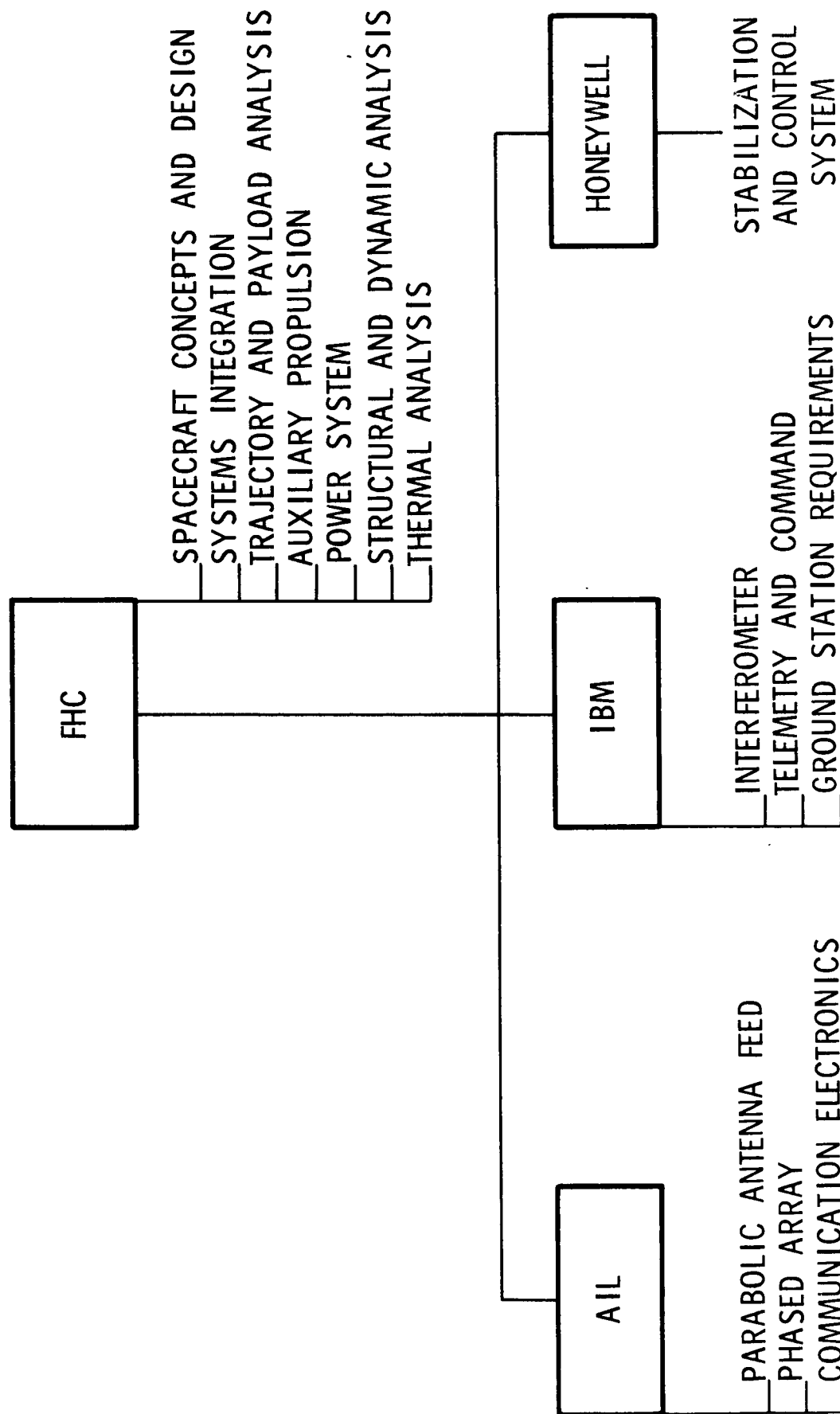
| Figure | Title                                                                        | Page |
|--------|------------------------------------------------------------------------------|------|
| 9.1-1  | Onboard System Data Flow, Interfaces to Ground Equipment                     | 9-4  |
| 9.1-2  | Ground Station Data Flow; Interfaces to Spacecraft and Other Ground Stations | 9-5  |
| 9.2-2  | Basic Commutation Configuration                                              | 9-15 |
| 9.2-2  | Data Handling System Configuration                                           | 9-18 |
| 9.2-3  | Telemetry Data Transmission System                                           | 9-25 |
| 9.2-4  | Telemetry Data Handling and Transmission Configuration                       | 9-33 |
| 9.2-5  | Block Diagram of Basic Telemetry Receiver                                    | 9-38 |
| 9.3-1  | Command Word Structure                                                       | 9-51 |
| 9.3-2  | Command System                                                               | 9-54 |
| 9.3-3  | Command Decoder                                                              | 9-55 |

## PREFACE

This report covers the efforts of Fairchild Hiller Corporation and its team of subcontractors on NASA Contract (NAS-W-1411). The team organization and responsibilities during the study effort are shown on the accompanying chart. The report is divided into eight volumes, as follows:

|          |                                           |
|----------|-------------------------------------------|
| Volume 1 | Summary                                   |
| Volume 2 | Systems Analysis                          |
| Volume 3 | Vehicle Engineering                       |
| Volume 4 | Power System                              |
|          | Orbital Analyses, Propulsion and Guidance |
| Volume 5 | Stabilization and Control                 |
| Volume 6 | Communication Experiments                 |
| Volume 7 | Radio Interferometer Experiment           |
|          | Telemetry and Command Systems             |
| Volume 8 | Program Budgetary Costs and Schedules     |

# ATS-4 TEAM ORGANIZATION



## 1.0 SUMMARY

### 1.1 OBJECTIVES AND JUSTIFICATION

Growth of the U. S. capability in space is dependent on the orderly evolution of supporting technologies. Realization of future plans and advanced programs presupposes the availability of requisite technology within a reasonable time frame and at a reasonable cost. Timely assessment of advanced technology followed by firm estimates of development feasibility, time, and cost are essential. When a given development is required to support several major programs, confidence in the proposed solutions becomes crucial. ATS mission objectives are addressed to the attainment of some of these critical goals within prescribed time and budget limitations.

The effectiveness of Government and Industry partnership in evolving practical solutions to major space problems is well attested to by the favorable and increasing success ratio of U. S. efforts. Fairchild Hiller Corporation and its subcontractors (AIL, IBM, Honeywell) believe the spacecraft study reported on herein constitutes an added example of this effectiveness. Each company has not only covered study aspects within its area of specialization but has also purposely contributed significant additional efforts through study, design and test tasks supporting the main program. In consequence, we are able to present the recommended spacecraft design approach as not only meeting mission objectives but also as representing the best technological approach to meeting the 1969-70 launch objectives with assurance.

The advanced Technology Satellite (ATS) series consists of experimental satellites whose principal objective is to demonstrate implementation of components, subsystems and techniques representative of the technologies required by many future utility and scientific satellite systems. The progressive development of technology by this series will support communications, navigation, meteorology and data acquisition applications.



ATS Mission-4 encompasses a giant step in the vital development and demonstration of a precision spacecraft stabilization and control system in conjunction with large aperture and multi-beam antennas of the type suited to communications, position determination and data acquisition with small terminals. For the purposes of this spacecraft study, a two year mission in equatorial synchronous orbit has been analyzed. The four principal experiments are:

- Deployment, pointing and utilization of a large parabolic antenna for simultaneous multi-frequency communications;
- Active spacecraft stabilization with possible augmentation by passive means;
- Deployment, pointing and utilization of a high gain, multi-beam, electronically steered array;
- Demonstration of a precision radio interferometer as a sensor for spacecraft attitude and/or antenna pointing reference.

#### 1.1.1 Utilization

Realization of this advanced technology embodied in the ATS-4 experiments is expected to be directly applicable to future systems for:

- Mass Communications - direct broadcast relay of FM and TV to remote areas;
- Civil and Military Communications Relay - fixed station point-to-point as well as mobile terminals such as manned satellites, aircraft, ocean shipping and portable ground terminals;
- Continuous Data Collection - Monitoring widespread, inexpensive sensors and transponders to assist in conservation surveys, weather prediction, air traffic control and oceanography.

- Space Mission Data Link - Wideband data links directly from manned space laboratories and relay of data from interplanetary and deep space missions without the interference of the earth's rotation or atmosphere.

Much of the world's population lives in underdeveloped areas remote from current means of rapid communications. Amidst the struggles of governments and ideologies, it is clear that the influence of rapid and reliable communications introduced into such areas could be decisive in the successful development of these peoples. The efficiency and effectiveness of government, the development of industry and commerce and the national security are all affected by the capacity, rapidity and reliability of a nation's communications network. Efficient communications can contribute to progress by dispelling ignorance, by coordinating businesses and by unifying the social and political aims of a people. It is a corollary that international understanding and cooperation among governments and peoples is aided by readily accessible communications.

Synchronous satellites offer unique advantages in the establishment of economical communications in a reasonably short time. At synchronous altitude, an equatorial orbit makes the land masses and population of a hemisphere constantly accessible to the satellite. High gain antennas with precision stabilization and control, such as those envisioned for the ATS-4, permit the ground terminals using the satellite to be simple, cheap and easily deployed. Roads, microwave towers, or expensive tropospheric installations will no longer be a prerequisite for communications to and from remote areas.

By the development of a communications system with the complexity restricted to the satellite, the opportunity arises to provide significant assistance to underdeveloped nations. The United States could contribute the fabrication, launch and in-orbit control of the satellite. Underdeveloped nations could utilize the satellite on a time or frequency shared basis without

the development of sophisticated facilities, provision of significant power or training of skilled maintenance personnel. Educational television, whose impact in underdeveloped countries will eventually dwarf its role in the U. S., could be made available in an air-dropped form to isolated villages. A community antenna, a rebroadcast station and solid state television sets sufficient for a small village could be packaged into a few crates suitable for delivery anywhere in the world.

#### 1.1.2 Implementation

The problems associated with deploying a controllable, large aperture antenna in space have been frequently discussed. Numerous studies have been conducted and estimates have been made regarding system weight and operational capability. However, to date, no large precision surface has ever actually been deployed in space or controlled (pointed) with the accuracy envisioned for the ATS-4.

Economical achievement of such a worthwhile goal requires development of the advanced technology proposed for ATS-4. Combining the advantages of a phased array and its inertialess multiple beam switching capability with a precisely-pointed, high gain parabolic reflector is an ingenious combination that could ultimately be operationally utilized for wideband, high data rate communications links between nations.

Focusing on the specific technological developments for ATS-4 spacecraft experimentation, evaluation of the multi-frequency feed and precision reflector stands out as a flight test necessity, as opposed to those items which can be evaluated by ground testing alone. For example, thermally induced distortions can be analysed in detail but never completely simulated on earth. The control system-structure interaction can be computer-simulated but not demonstrated in a gravity environment.

The spacecraft control system accuracies needed have never been demonstrated for an earth pointed vehicle. Perfection of this system is

ultimately required if the full advantages of a synchronous satellite are ever to be properly exploited. Hand-in-hand with the stabilization system is the development of an interferometer reference system that can ultimately surpass accuracies of the optical attitude sensors that represent the present state of the art.

The four principal experiments properly integrated into a single spacecraft represent a meaningful challenge for advanced engineering. The phased array complements the parabolic antenna while the interferometer provides a back-up for the attitude reference system. In the configuration proposed, the antenna and stabilization system are tied together in a monopulse system and the phased array can double as an emergency reference system. In this way, experiment redundancy is achieved and a 2-year life expectancy enhanced. Similarly, with all four experiments on one spacecraft, NASA can choose which combination will best satisfy applications for achieving new national goals in the decade ahead.

## 1.2 PROGRAM FEASIBILITY

The study has proven the feasibility of accomplishing the ATS-4 mission and program objectives. However, since the study was conceptual and analytical in nature, additional subsystem developments are essential to fully validate the selected approach. Program Feasibility and the necessary developments are discussed in the following sections in terms of the four basic experiments that comprise the spacecraft.

### 1.2.1 Parabolic Antenna

Reflector - The design of the precision reflector received heavy emphasis during this study. After considering several alternatives, a petal system with unique features has been selected which insure surface accuracy in the changing orbital thermal environment. These features include the use of a superinsulated truss sub-structure for the petals combined with a segmented floating mesh reflecting surface. This combination has been analyzed in detail and found to meet the demanding X-band surface accuracy requirements. Concept feasibility has been analytically proven during this study but significant development testing remains to insure flight reliability. NASA has taken the first steps in this direction by the initiation of a separate reflector development program. Nevertheless, the FHC studies have shown a great inter-relationship and dependency between the reflector design and the complete spacecraft concept. On the basis of the extensive studies reported on in this document, it is Fairchild Hiller's belief that the results of the ground test development program of the large parabolic reflector cannot be fully exploited, unless the concept is compatible with the required spacecraft configuration. Launch dynamic loads, control system/structure interaction, deployment system and thermal distortion are all significantly affected by the configuration. A reflector program divorced from the spacecraft concept will yield useful results but it cannot serve as the prototype of the final mission reflector.

The spacecraft reflector free-free structural mode shapes and frequencies have been determined. The first structural frequency is 6.52 rad/sec (1.04 cps). A control system simulation which compared the response of an infinitely rigid body with the predicted flexible structure showed no difference in response in the critical dynamic stability region. This analysis verified the design approach and feasibility of stabilizing the flexible reflector structure to the required accuracy. A reasonable dynamic stability margin has been analytically demonstrated.

Feed System - The parabolic antenna multiband feed consists of simple dipoles for the UHF and VHF bands, broad-band dipoles for S-band, and waveguide horns for X-band. The individual radiating elements are optimized with respect to height above ground plane, droop angle, separation between elements, etc. The major question concerning feasibility of the parabolic antenna feed was the amount of blockage caused by the feed mast. Experimental determinations of mast blockage showed acceptable values (1 to 2 db) realized at this time. These values can be improved on by further development.

Interaction between the various elements of the feed is not a critical feasibility question. Because of the large frequency separation between bands, and with the use of crossed polarization, inter-element coupling can be held to an acceptably low value.

A unique feature of the proposed configuration is that the antenna directly provides sensor inputs for the control system by use of an X-band monopulse. The monopulse feed is of conventional design and no questions concerning its feasibility exist. The precise amount of tracking error introduced into the difference mode pattern by the adjacent feeds and by the mast will be determined experimentally.

Further engineering development needs to be done, to determine the monopulse tracking error and to minimize feed interaction. A scale model of

the multiband feed, a feed network, and a combination parabolic reflector and feed support structure should be designed. The paraboloid need not simulate the deployable properties of the full-scale reflector. The scale model system will be used as an engineering device to obtain the RF design information required to construct a full-scale antenna system. The information is primarily geometrical in nature giving the size, number, location and orientation of the elements comprising the feed. Parameters such as the radiation pattern, polarization, feed coupling and impedance are to be measured. Some preliminary scale-model work directed at the design of the feed support structure has already been performed and is described in Section 7 of this report.

The scale factor of the model will be determined by trade-offs amongst equipment availability, accuracy of simulation, range availability and cost. Measurements will be divided into two parts. The first part will be concerned with the feed separately and will provide the feed design data; of prime importance are the X-band and 100 MHz feeds which are the most difficult to analyze. The second part of the program will join the feed and the feed support structure to provide data for the design of the feed support structure. Finally, the overall performance of the complete antenna system will be measured when the feed and its support structure are joined to the paraboloid.

#### 1.2.2 Stabilization and Control System

The feasibility of precision spacecraft pointing to any point on the earth's disc to within  $0.1^\circ$  has been analytically demonstrated. The selected system is also capable of tracking at a rate of 10 milliradians per minute with an accuracy of  $0.5^\circ$ . The most significant additional development effort is related to sensor accuracies and required fields of view.

After considering several alternatives, the selected attitude reference system consists of an electronically gimbaled horizon sensor and Polaris star

tracker. The study revealed that there are no off-the-shelf sensors to meet the mission pointing and accuracy requirements, although current designs with moderate modifications appear feasible. With regard to the use of a Polaris star tracker, no one has built and flown such a device as a yaw angle sensor. Polaris is a rather dim star (Mag +2.1) and is considered for this application only because of its uniquely advantageous position relative to the orbit plane. Use of any other brighter star requires significant gimbaling and coordinate transformation, as well as resulting in daily occulting and hence loss of reference. The JPL-designed Canopus tracker for the Mariner program is a single axis device with  $+17^\circ$  electronic gimbal freedom in the nonsensitive axis and an instantaneous field-of-view of  $6^\circ$  by  $9^\circ$ . This tracker meets many of the system requirements; however, modifications are required in the star magnitude gate, a reduced instantaneous field-of-view to limit stray light and a means of compensating for the apparent diurnal motion of Polaris.

The horizon scanner which best meets the system requirements for pitch and roll angle sensing is a combination of the Apollo and MOGO designs developed by ATD. This design employs a double positor and two mirrors in each of two axes through a single set of optics to provide vehicle offset pointing to any location on the earth disc and beyond (to  $\pm 15^\circ$ ) without any field-of-view obstruction from the second mirror. Throughout the offset pointing maneuvers, the optical axes of the scanner continues to chord scan through the center of the earth. Using this approach, analysis indicates that the attitude measurement error of the sensor will be on the order of  $0.06^\circ$ . This figure, which includes the horizon definition uncertainty of 10 seconds at synchronous altitude will enable the specified pitch and roll pointing accuracy requirement of 0.1 degree to be met. The primary errors in the horizon scanner are due to electronic component stability and thermal stability as the optical axis is pointed toward and away from the direction of the sun each day. Since thermal isolation cannot



be completely achieved, thermal stability of the optics is a key problem requiring study and test.

A combination inertia wheel-reaction jet torqueing subsystem has been selected to provide proportional control without a finite deadband. This reduces the number of jet pulses to those required for wheel unloading and specific larger maneuvers. A comparable all-jet system would have to provide nearly 1,000,000 pulses per axis in a two year period. No reaction jet system has ever met this kind of a life-cycling requirement.

The selected wheel system is flight proven and similar to the OAO system. Considerable development work has been accomplished on low thrust hydrazine systems and no serious problems are anticipated with this design.

The critical factors governing the feasibility of the electronics and the SCS controller are basically component stability and reliability. The recommended SCS controller is essentially a special-purpose digital computer, designed to perform the stabilization and control function. To assure feasibility, life test data on critical components and piece parts is required to determine the degree of degraded performance as well as discrete failure rates due to thermal variations, power cycling and time. A redundancy optimization study will also be necessary to determine the form and degree of redundancy required to meet the reliability goal.

In the current ATS-4 study, each of the SCS subsystems were examined independently to determine the feasibility of their application to the ATS-4 program. The complete system was then examined using a computer simulation, to evaluate the interaction of the control system with the flexible satellite structure. It was determined that the natural frequency of the roll and pitch axes with a rigid structure is 0.46 radian/sec and 0.67 radian/sec, respectively. In comparing the rigid versus the flexible responses, there is little difference

in the response below 4 radians/sec. Likewise, there is an insignificant difference in control system response for varying structural damping coefficients. The separation between the control system frequency and the first structural bending mode is more than three octaves. With this degree of separation no control problem was evident during the simulation and none is anticipated, particularly in view of the compact nature of the proposed configuration with sensors and torquers located in close proximity in the same module.

### 1.2.3 Phased Array

After investigating a number of phased array configurations, it has been determined that the corporate-fed phased array provides the most versatile, efficient and reliable electronic scan system. The technique can be implemented, in the laboratory, with currently available hardware. The ferrite phase shifters, which will be used for beam switching, are temperature sensitive and need further investigation. Techniques to control and reduce the effects of temperature variations on the ferrite characteristics need exploration. Thermal control of the spacecraft (or of the phased array electronic package) needs further study.

Areas for further investigations are as follows:

- Design and construction of individual components such as phase shifters, quadruplexers, circulators, and drivers and subsystems of these components to determine and optimize their performance under the conditions of the space environment.
- Pursue component improvement by undertaking development of ferrite phase shifters, drivers, and waveguides. The areas of improvement in the phasors and waveguide would be primarily the reduction of size and weight. Advantage can be taken of the modest requirements of this application, such as narrow RF bandwidth, to improve system performance, e.g. loss, temperature sensitivity, and ferrite drive power.

- Measurement and optimization of beam patterns in relation to individual element behavior, arrangement and spacing of elements, aperture size and aspect ratio.

#### 1.2.4 Interferometer

Results of the study indicate that a direct phase reading X-band radio interferometer is capable of determining spacecraft attitude (pitch and roll) to an accuracy of better than  $\pm 0.05$  degree by the use of state-of-the-art components. This accuracy can be improved by incorporating filters which are used in conjunction with the associated processor. Accuracy is obtained by employing signal-to-noise ratios of 30 db or greater and by using a superinsulated aluminum box beam for the interferometer arms (which minimizes phase errors that can result from bending or expansion). The interferometer arm assembly is the most critical subassembly in the interferometer. However, preliminary analysis indicates that by applying well-known mechanical and thermal design techniques, residual inaccuracies can be made acceptably small. Instrumentation error, such as electrical phase errors due to variation in cable length, are reduced by performing amplification and conversion near the antenna location.

### 1.3 SUBSYSTEM SUMMARIES

#### 1.3.1 Configuration Description

The spacecraft concept Fairchild-Hiller is recommending for the ATS-4 mission is shown on Figures 1.3-1 and 1.3-2. The vehicle is launched by an Atlas SLV-3C/ Centaur booster and housed inside a modified Surveyor Shroud. The vehicle is spin stabilized in the transfer orbit and apogee injection is accomplished by the TE-364-3 (Improved Delta) solid rocket motor.

The large parabolic reflector is formed by the deployment of 32 rigid petals which rotate about a skewed axis to facilitate stowage in the available volume. The concept represents an "inverted" configuration since the petals are hinged to fold down (toward booster) instead of the conventional upward hinged motion. This results in a lower launch C. G., lighter feed support mast, and a solar panel configuration which is more readily adaptable to pre-orbital solar power. The C. G. in the orbit configuration is within the spacecraft module, permitting an APS (auxiliary propulsion system) installation which requires no re-orientation for the station keeping modes.

A solar cell-battery combination comprises the power system. The solar panels are fixed in a cruciform arrangement attached to the tips of two sets of opposite reflector petals. The solar panel support petals are stiffened to achieve a spacecraft natural frequency above 1 cps. Solar cells are attached to both sides of the sub-structure and provide approximately 310 watts of primary power to the load bus. Fixed panels were chosen over rotating panels for simplicity and improved reliability. The panels are "wrapped around" the folding petals during launch. This will result in a worst case solar vector angle relative to the vehicle spin axis during the transfer orbit of  $20^{\circ}$ . Using the non-degraded value of solar cell output and an 85% power conversion efficiency results in a pre-orbital power capability of 64 watts for an equinox launch and 130 watts for a solstice launch. Changing the fixed panels to rotating panels (for more ambitious missions and with the equivalent deployed structural area)

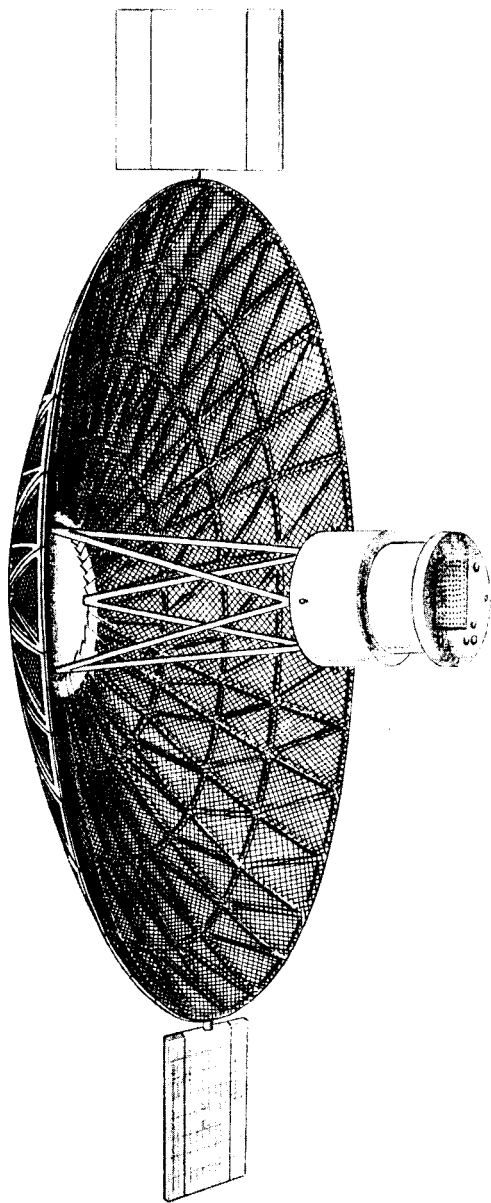
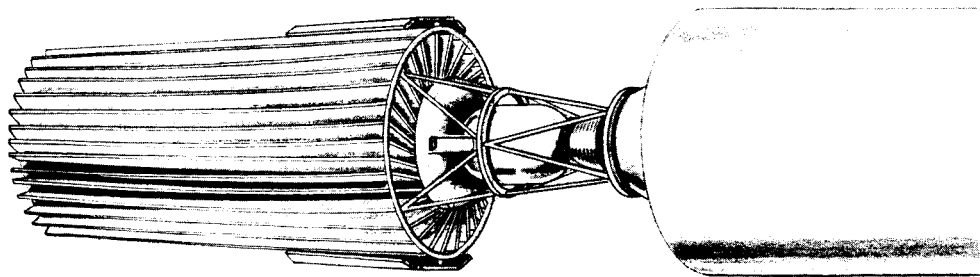
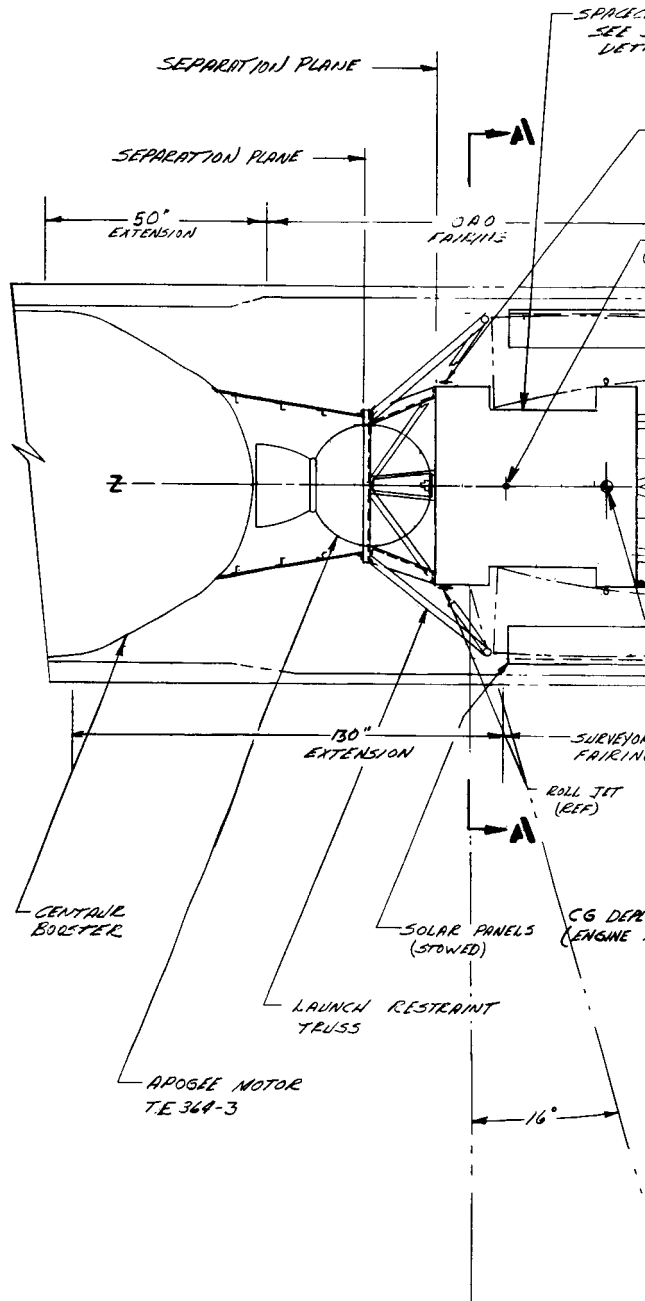


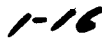
FIGURE 1.3-1 FAIRCHILD HILLER ATS-4 CONCEPT



|       | BEFORE<br>FIRING<br>APOGEE<br>MOTOR | DEPLOYED |
|-------|-------------------------------------|----------|
| $I_x$ | 1140                                | 2150     |
| $I_y$ | 1140                                | 1226     |
| $I_z$ | 303                                 | 1677     |

SLUG FT<sup>2</sup>





[REDACTED]

will increase their power output by 50% (150 watts) with a 25% (25 lb.) reduction in weight. Similarly for the existing power profile a 50% (50 lb.) weight saving is possible for oriented panels.

The spacecraft module and apogee injection motor are attached to the standard Centaur interface by a short conical adaptor. A single module is used for all equipment, experiments and sensors with significant volume available for additional experiments. A six-tube truss is provided to support the reflector hub and the petal hinges.

The attitude control jets are positioned around the circumference of the spacecraft module. Two roll and two pitch jets in combination with four yaw jets are provided for in-orbit acquisition maneuvers, unloading of the inertia wheels and stabilization during the auxiliary propulsion thrusting modes. The roll jets are placed below the Polaris star tracker to eliminate any optical problems. All the jets are arranged to thrust away from the reflector.

The APS (auxiliary propulsion system) consists of three horizontally oriented nozzels aligned through the C. G. Two of the nozzels provide east-west repositioning capability while the third nozzle is capable of north-south station keeping. One nozzle is sufficient for this mode since by choosing the burn compatible with the proper nodal crossing either a + or - inclination correction is possible without vehicle reorientation.

Figure 1.3-3 depicts the spacecraft module in greater detail. The phased array, interferometer elements, and horizon sensors are on the earth-facing side and clear of any obstruction after the apogee motor is jettisoned. The phased array consists of 64 horn elements forming a 36-inch x 31-inch planar array. The interferometer elements consist of five horn antennas mounted to a superinsulated "L" beam.

The truss structure which restrains the reflector petals during launch launch is jettisoned with the apogee injection motor. This is a unique fall-out of this concept and eliminates the need for an additional separation device.



The transfer orbit and apogee injection attitude control thrusters are attached to the launch restraint ring. This structure also contains the associated control fuel supply and mounts the de-spin yo-yo. Separation of the apogee engine and launch restraint truss is accomplished by the firing of four explosive bolts.

The spacecraft in-orbit weight is 1351 pounds; a 254 pound payload margin exists for additional experiments. A weight breakdown is shown in Table 1.3-1.

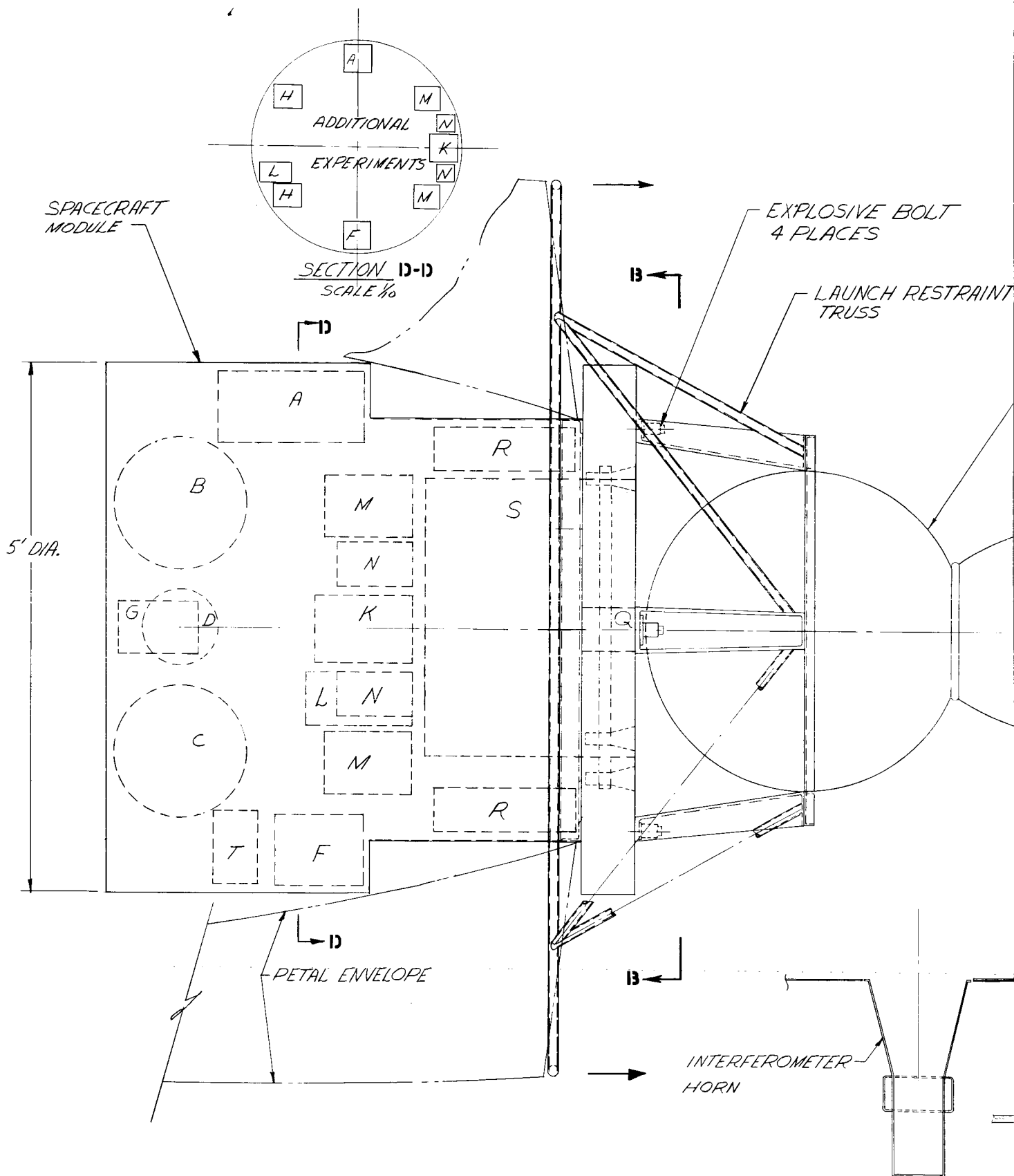
TABLE 1.3-1 SPACECRAFT WEIGHT SUMMARY - ORBITAL CONFIGURATION

|                                                      | <u>Weight (lb.)</u> |
|------------------------------------------------------|---------------------|
| Reflector (Including Deployment System, Locks, Etc.) | 274                 |
| Stabilization and Control                            | 192.8               |
| Auxiliary Power System                               | 172                 |
| Phased Array                                         | 166                 |
| Interferometer                                       | 30.5                |
| **Solar Panels (Fixed)                               | 103.0               |
| Battery And Power Conditioner                        | 77                  |
| Feed Mast                                            | 46                  |
| Communication Equipment                              | 55                  |
| Structure And Mechanism                              | 150                 |
| Telemetry, Command & Tracking                        | 40                  |
| Cabling And Miscellaneous                            | 30                  |
| Feed                                                 | 15                  |
|                                                      | <hr/>               |
| TOTAL                                                | 1351.               |
| Additional Experiment Payload Capability             | <hr/> 254           |
| Maximum Payload                                      | 1605                |

\*\*Oriented Solar Panels Weight 50 Pounds Instead of 103 Pounds For The Same Power Output.

### 1.3.2 Parabolic Reflector

The parabolic reflector is formed by the deployment of 32 rigid petals which rotate about a skewed axis. Each petal consists of a trussed



| PACKAGE |                    |
|---------|--------------------|
| A       | STAR TRACKER       |
| B       | PROPELLANT TANK    |
| C       | REACTION FUEL TANK |
| D       | NITROGEN TANK      |
| E       | REACTION WHEELS    |
| F       | POWER INVERTER     |
| G       | 3 AXIS GYRO        |
| H       | COMMUNICATION SYS. |
| J       |                    |
| K       | INTERFEROMETER     |

| PACKAGE |                    |
|---------|--------------------|
| L       | ACS CONTROL "R"    |
| M       | TELEMETRY          |
| N       | DATA SYSTEM        |
| P       |                    |
| Q       | HORIZON SENSOR     |
| R       | BATTERY            |
| S       | PHASED ARRAY       |
| T       | POWER CONDITIONING |

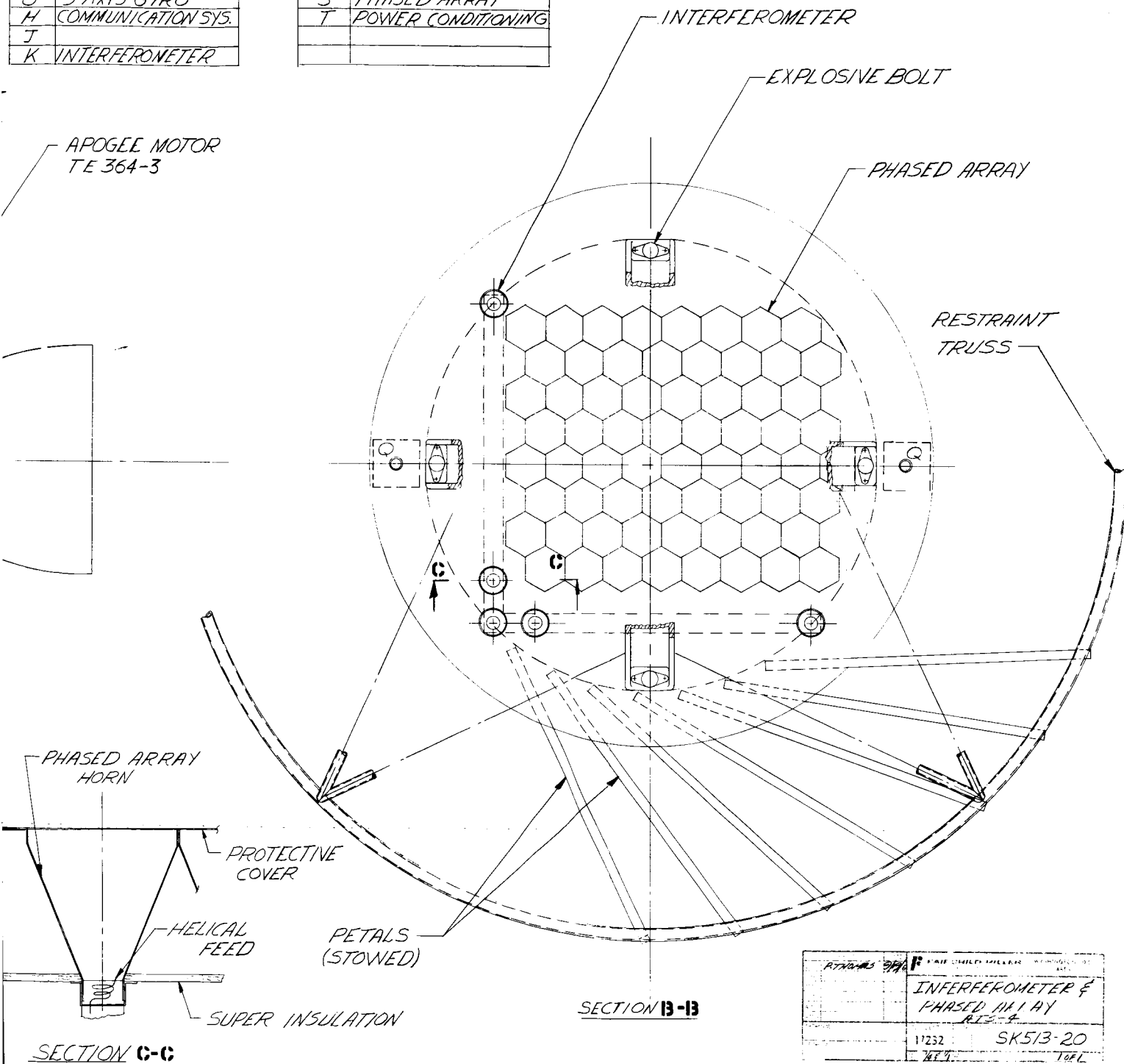


Figure 1.3-3 Spacecraft Module Detail

frame which supports a formed "floating" reflector mesh. The structural petal beams are fabricated from rectangular aluminum tubing and wrapped in super-insulation to reduce their temperature gradients and excursions. This technique reduces the "worst case" thermal distortion to less than .070 inches. The reflecting surface is formed by an adjustable, segmented mesh which is required to "float" in its contoured shape since even relatively small temperature excursions (of the order of 50°F) will cause deformation far beyond permissible tolerances if the mesh is fixed relative to its supporting substructure.

Torsion springs are provided to supply the deployment energy. The petals are locked at the hinge in the deployed position by means of a spring loaded ball-lock pin which is mechanically sequenced by petal rotation. Each petal is provided with an adjustable stop which insures the "extended conformity" of the petal system. A crank is attached to the petal hinge which serves as the attachment point for a pushrod.

The pushrods from each petal are tied to a centrally mounted wheel which serves as the deployment synchronizer for the petal. By means of a centrifugal governor, the deployment rates are retarded to a level which will insure a smooth-locking action without prohibitive inertia loads; it is also possible to use an electric motor instead of a mechanical governor to control the deployment velocity and at the same time serve as a redundant deployment device. The latter type of system was used successfully on the PEGASUS deployment system.

In addition to the hinge lock, each petal will be locked to its adjacent petal at the rim to insure ring continuity of the deployed reflector. The lock will incorporate a capability permitting relative radial growth between petals caused by petal temperature differences.

This reflector structure has been studied in detail by means of a dynamic response analysis. In the launch configuration, the petals are

supported at the hub, near their mid-point, and at the tips. This support arrangement results in a launch natural frequency of more than 7 cps and a stress level (due to launch amplifications) of less than 20,000 psi. When deployed, the free-free spacecraft/reflector natural frequency is 1.04 cps.

The weight of the reflector including deployment system and all locks is 274 pounds.

### 1.3.3 Parabolic Antenna Feed

The parabolic antenna feed is a multifrequency antenna and feed system consisting of four separate groups integrated into a single package and mounted at the focus of the paraboloid. (Figure 1.3-4)

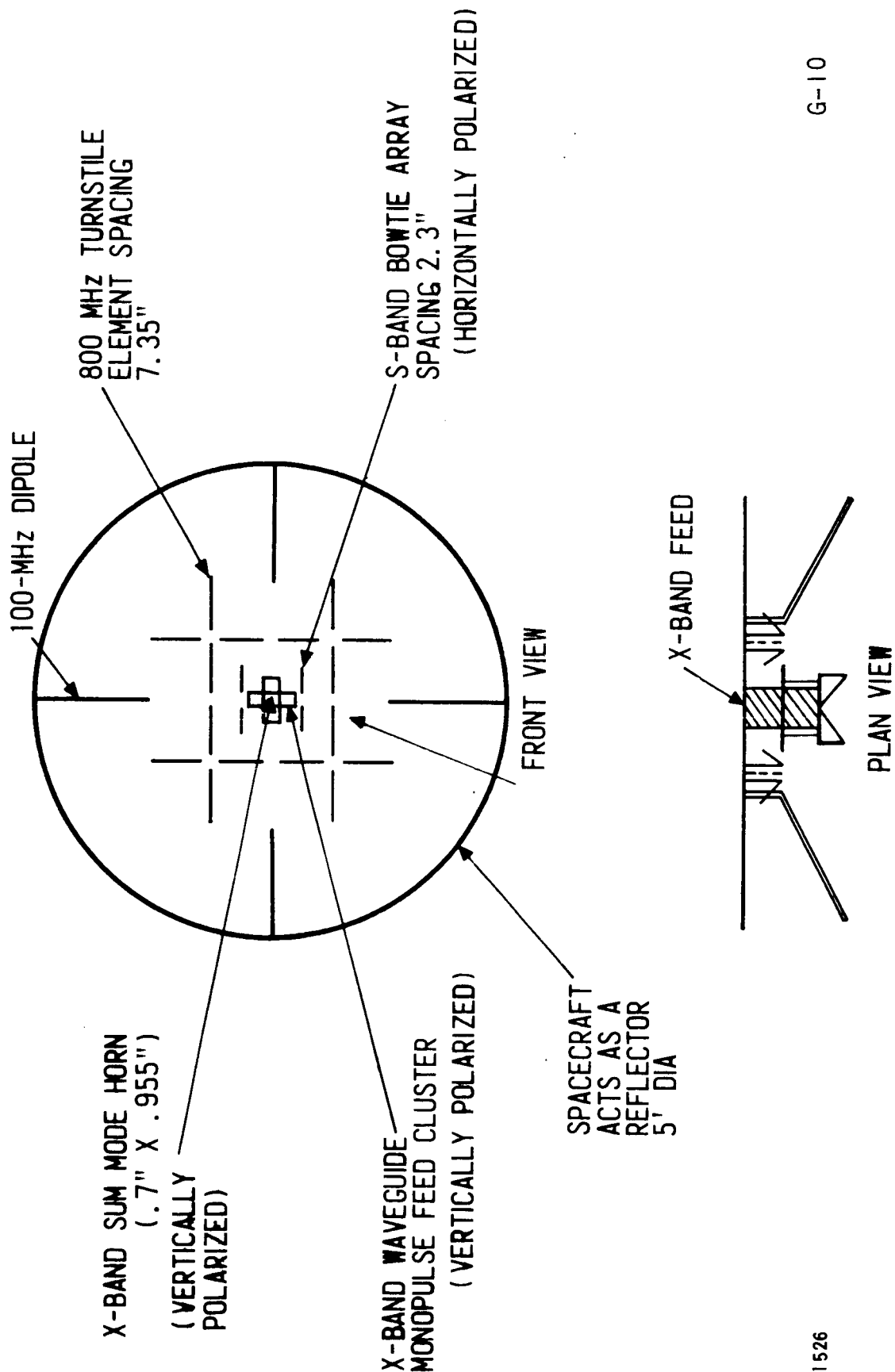
X-Band Feed - The X-Band feed is a linearly-polarized five-horn monopulse cluster. The center horn is used for transmission and reception, at 7.3 GHz and 8.0 GHz, respectively, in the sum mode. Monopulse difference signals will be received on the outer pairs of horns at 8.0 GHz. The azimuth and elevation difference signals are derived from two waveguide E-plane T junctions. The size, spacing and the layout of the five-horn cluster is dependent upon the type of monopulse optimization selected.

S-Band Feed - The S-Band feed is a two-element array of bowtie dipole elements. In order to achieve a small element spacing the elements have been cross polarized with respect to the X-band horn cluster and placed in front of it. The array parameters which will be used for pattern control are the distance in front of the horn cluster, the distance between the two elements, and the included and "droop" angles of the bowtie elements. Drooping the bowtie elements tends to broaden the radiation pattern by increasing the radiation intensity in the direction parallel to the ground plane.

800 MHz Feed - The 800 MHz feed consists of a 4-element array of turnstile elements mounted over the ground plane provided by the spacecraft electronics package. The turnstile elements are "crossed" dipoles

Figure 1.3-4

# MULTIBAND PRIME FOCUS FEED



which are fed in time quadrature in order to obtain circular polarization. The parameters for control of the pattern of this feed are the element spacing, the height above the ground plane, and the droop angle of the dipoles.

100 MHz Feed - The 100 MHz feed is a turnstile antenna mounted over the ground plane provided by the spacecraft electronics compartment. Pattern control is obtained by adjustments of the height above the ground plane and the droop angle of the elements. Since the ground plane is electrically small at 100 MHz, its size has been increased by the addition of "spokes" at the outer edge of the compartment.

#### 1.3.4 Attitude Stabilization and Control System

The ATS-4 Stabilization and Control System (SCS) consists of sensors, torquers, (moment producers) and a system controller. The sensors include a two-axis horizon scanner of the double mirror dithered positor type for pitch and roll angle sensing, a single axis Polaris star tracker similar to that used on the Mariner program for yaw angle sensing, coarse and medium fine sun sensors for attitude sensing during acquisition, and a three-axis gyro reference unit to be used during certain maneuvers and control modes.

The horizon scanner is used for initial earth acquisition and to provide vehicle pitch and roll reference. In order to offset point the antenna to a specific ground station or to a horizon location for close-earth satellite acquisition, the horizon scanner chord-scan center pulse, being a digital device, is biased off to provide the required offset point signal to the autopilot. In the event the horizon sensor performance becomes degraded, the X-Band monopulse system can be used to point the spacecraft towards the desired ground station if it comes within  $0.15^{\circ}$  of the required offset point. While holding a ground station offset point, the X-band monopulse system normally provides the autopilot steering commands and is capable of holding the spacecraft to an accuracy of  $0.05^{\circ}$ . However, if the horizon scanner is used to hold the offset point attitude, a figure 8 bias (associated with the residual inclination error) must be incorporated in the scanner command

signal through the SCS controller. The magnitude of the inclination must be determined from ground track and received by the controller through the data command link. Alternately, when the gyro reference unit provides attitude control while holding an offset pointing attitude, the orbital rate must be incorporated into the gyro bias as well as the figure-8 bias.

Since Polaris is 50 minutes removed from the celestial north pole, there is an apparent diurnal motion of Polaris which requires biasing the star tracker yaw axis. Similarly, when performing roll offset maneuvers, the star reference axis relative to the vehicle yaw axis is electronically gimbaled to prevent loss of the star.

In the planned ATS-4 mission profile, the gyro reference unit is operated only about 500 hours out of the two-year period. The selected gyro is the Honeywell GG 334C gas-bearing gyro which has a 90-day drift stability of  $0.1^{\circ}/\text{hr}$   $3\sigma$  stable to  $0.01^{\circ}/\text{hr}$ . This gyro has been built and tested with 10,000 spin motor start-ups without noticeable wear or failure. In the planned mission profile, the gyro reference unit is used during ascent and injection, acquisition, and antenna pattern measurement maneuvers. It also serves as a backup to the horizon scanner and for calibration of the monopulse systems.

A three-axis inertia wheel system (ac) is used to provide proportional attitude control without a finite deadband during fine attitude pointing. Hydrazine monopropellant reaction jets with the Shell 405 catalyst will be used for wheel unloading and initial acquisition. The jets have been sized at 0.03 pounds and require 3900 lb-sec impulse for the two-year mission. Cold gas and hypergolic bipropellants were considered but eliminated on the basis of system weight and reliability. The AVCO and GE resisto jets also were discarded due to very high power requirements (200 to 400 watts power on demand). The only way to use the AVCO or GE resisto jet would be on a long moment arm (at the edge of the antenna) and at a lower thrust



level. This, however, required flexible fuel line joints to permit deployment. Additionally, if the jets were on the antenna rim, the complete vehicle dynamics must be incorporated into the inner loop of the control system producing possible instabilities. TRW, however, has a continuously heated resisto-jet design which requires much less power and could be considered feasible for the thruster requirements established, for this application. Hydrazine monopropellant systems have been built and tested at the desired thrust level. Of the two feasible approaches (TRW decomposed ammonia resisto-jet and hydrazine monopropellant) the hydrazine system has had more development testing and requires less power -- although the resisto-jet has a higher  $I_{sp}$ . Since the APS will be using hydrazine the advantage of commonality in fuels also contributes to making the hydrazine approach more attractive.

The reaction jet system has six jets (2 in pitch, 2 in roll and 2 in yaw) in the primary system and six in the redundant system mounted on 2.5 foot moment arms and developing 0.03 pound thrust. The yaw jets, however, have split nozzles providing two 0.015 pound thrust outputs from one valve for a matched pair. The thrust on-time for wheel unloading is 10 seconds in pitch and 12.5 seconds in roll and yaw. In the two-year period, there will be about 10,000 pulses in all three axes for a total impulse requirement of 3900 lb-sec.

The system controller contains all the control logic, mode switching sensor commands, redundancy diagnostics, experiment logic and system monitor logic. This controller, which serves as the electronic interface between the sensors and moment producers, is a digital device with both digital and analog input and output capability.

The system is capable of nadir and offset pointing to an accuracy of  $0.1^\circ$  in pitch and roll. The major errors in the pointing system are in the horizon scanner alignment, thermal stability and electronics life -- resulting in a 0.06 degree contribution to the pointing error. Wheel hang-off error can be as high as 0.04 degree but this occurs only during wheel unloading (about once every 12 hours.) While holding attitude via the monopulse

signals, pointing accuracy may be as precise as 0.03 to 0.04 degree except during wheel unloading when it is degraded to 0.052 degree (pitch and roll). The yaw pointing error of 0.2 degree, being considerably less stringent, can be easily met.

A block diagram of the overall stabilization and control system is shown in Figure 1.3-5. The complete system, including necessary redundancy, weighs 193 pounds and requires an average power of 88 watts.

#### 1.3.5 Launch Vehicle - Ascent and Orbit Injection

Of the three launch vehicles specified for consideration for the ATS-4 mission (SLV 3A/Agena, SLV 3C/Centaur, and Titan III C) only the latter two were subjected to a final trade-off analysis and comparison as being generally compatible with the payload weight-volume requirements. In order to meet these requirements, a separate apogee injection stage and an extended Surveyor shroud were considered for the SLV 3C/Centaur; no apogee stage was needed for the Titan III C but the use of a modified OAO shroud, in lieu of the smaller standard shroud, was assumed.

The apogee injection stages studied for the SLV 3C/Centaur included two versions of the 3-axis stabilized Burner II, the BII-027B, incorporating the TE 364-3 solid rocket motor (Improved Delta Model) and the BII-128B with the TE 364-4 extended rocket motor. Spin-stabilized stages using these same solid rocket motors were also considered.

As shown in Table 1.3-2, the Titan III C has a markedly higher payload weight capability in addition to the advantage of requiring no apogee stage. However, the SLV 3C/Centaur with a spin-stabilized TE 364-3 motor has a much lower cost and still provides a significant additional experiment payload capability. Hence, this launch vehicle-apogee injection stage is recommended for the ATS-4 mission. Should additional payload capability be desired, the TE 364-4 motor could be employed with a moderate increase in launch vehicle cost.

TABLE 1.3-2

**BOOSTER DATA**

| BOOSTER                                                              | APOGEE STAGE<br>OR ENGINE | GROSS ORBIT<br>PAYLOAD<br>(2ND APOGEE) | BOOSTER AND<br>APOGEE STAGE<br>COST | WEIGHT FOR ADDITIONAL<br>EXPERIMENTS<br>(1,350 LB S/C) |
|----------------------------------------------------------------------|---------------------------|----------------------------------------|-------------------------------------|--------------------------------------------------------|
| SLV 3C/CENTAUR<br>WITH 10 FOOT<br>EXTENSION OF<br>SURVEYOR<br>SHROUD | B-II 027B                 | 1,265 LB                               | \$16.9 M                            | —                                                      |
|                                                                      | B-II 128B                 | 1,400 LB                               | \$18.4 M                            | —                                                      |
|                                                                      | TE-364-3                  | 1,605 LB                               | \$13.7 M                            | 255 LB                                                 |
|                                                                      | TE-364-4                  | 1,790 LB                               | \$14.8 M                            | 440 LB                                                 |
| TITAN 3C WITH<br>MODIFIED OAO<br>SHROUD                              | —                         | 1,865 LB                               | \$17.6 M                            | 515 LB                                                 |

TITAN 3C  
 \$2.1 M 2 YEARS PRIOR TO LAUNCH  
 \$9.4 M 1 YEAR PRIOR TO LAUNCH  
 \$6.1 M YEAR OF LAUNCH  
\$17.6 M TOTAL

SLV-3C/CENTAUR  
 \$4.7 M YEAR PRIOR TO LAUNCH  
 \$8.7 M YEAR OF LAUNCH  
\$13.4 M TOTAL

BURNER II  
 -027B - \$3.50 M  
 -128B - \$5.00 M

TE 364-3 - \$0.3 M  
 TE 364-4 - \$1.4 M

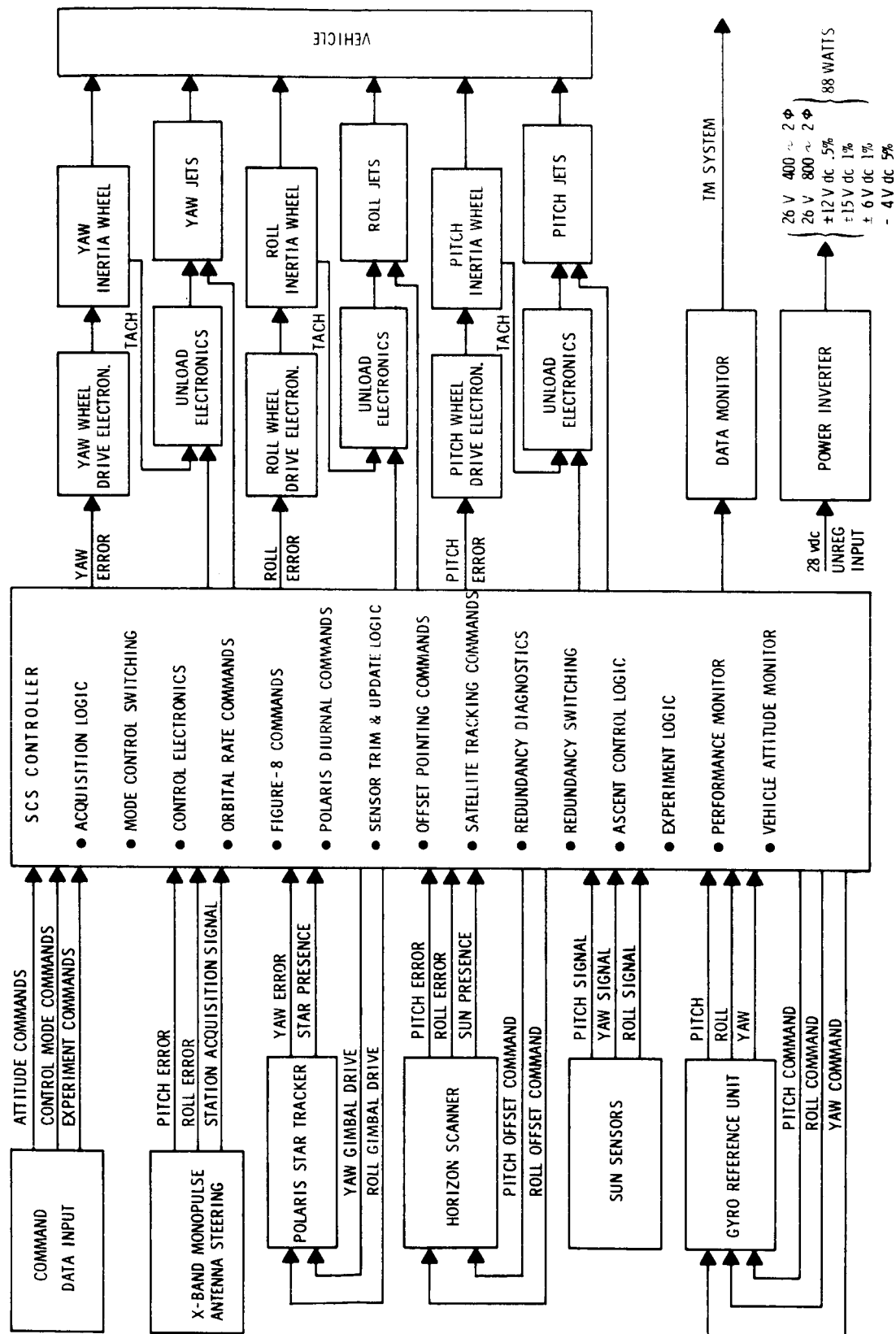


FIGURE 1.3-5 SCS BLOCK DIAGRAM

The choice of an ascent trajectory and final orbit injection procedure was based upon a consideration of such factors as: operational flexibility of the launch vehicle in the ascent trajectory; ground tracking facilities for monitoring (and possible control) during ascent and orbit injection; minimizing, determining and correcting orbit injection errors; and effectiveness and ease of satellite checkout and initial experimentation following injection, prior to repositioning at its operating longitude station(s).

The selected ascent trajectory and final orbit injection procedure is depicted in Figure 1.3-6 based on a due-East launch from ETR. For this recommended approach, using a spin-stabilized TE 364-3 solid rocket motor as an apogee injection stage (AIS), the Centaur would provide a  $7.6^{\circ}$  plane change (inclination reduction) at its second burn which initiates the transfer orbit. The Centaur vehicle would then rotate (yaw) in essentially the local horizontal plane so as to orient the thrust vector of the AIS in the required direction for the apogee injection impulse. During the subsequent coast period in the transfer orbit and the final orbit injection maneuver, the pre-orbital spin control system acts to preserve the desired inertial orientation of the spin axis.

Upon reaching the second apogee of the transfer orbit (nominally 16.2 hrs. after launch) ignition of the apogee injection stage is commanded from the ground in order to achieve the final 24-hour equatorial orbit. The injection longitude station is  $54^{\circ}$  West.

Correction of initial orbit injection errors is accomplished within 2 to 24-hours after injection, following attainment of the nominal Earth-pointing orientation by the attitude control system. Following initial satellite checkout and experimentation, the ATS-4 will be repositioned near  $90^{\circ}$  West longitude for more facile control by the ATS-4 stations at Mojave and Rosman.

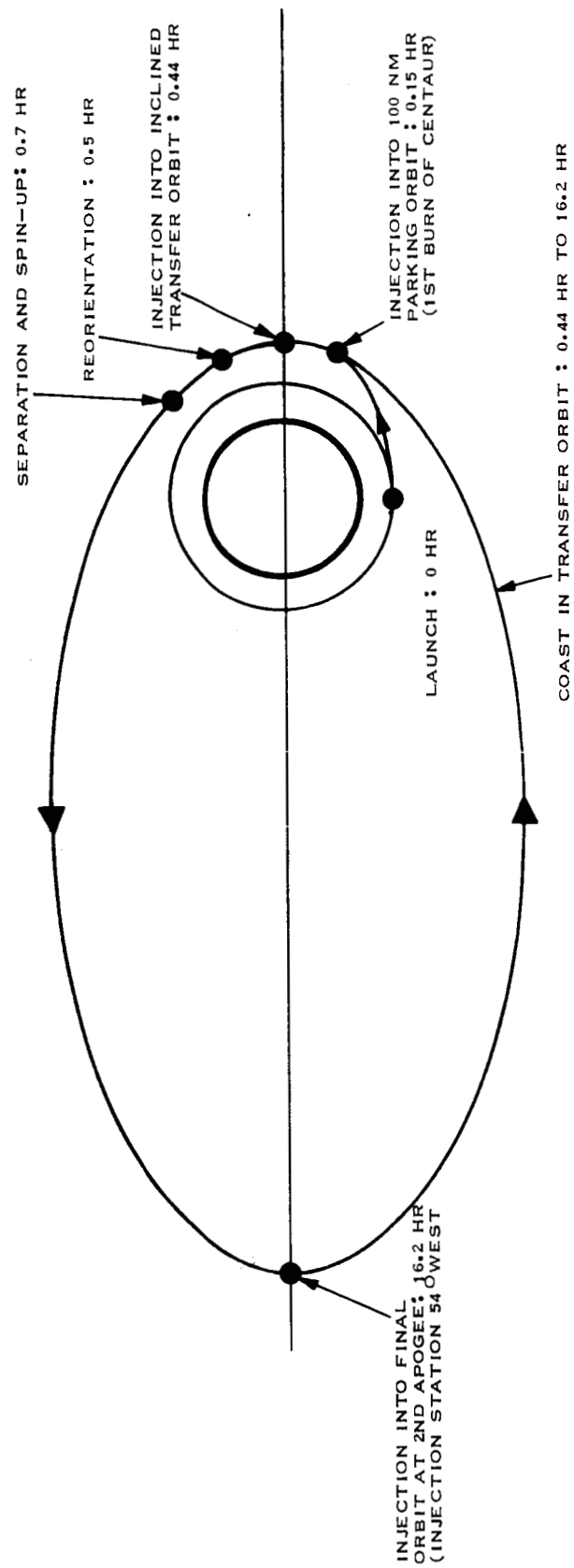


Figure 1.3-6 ATS-4 Ascent Trajectory

### 1.3.6 Interferometer System

One of the principal experiments of the ATS-4 mission will be the demonstration of a precision radio interferometer as a sensor for spacecraft attitude and/or antenna pointing reference. The pointing accuracy of the interferometer must be  $\pm 0.1$  degrees or better in order to be used as a reference for the parabolic antenna experiment. Thus, the design objective is to achieve an accuracy of  $\pm 0.05$  degrees about the roll and pitch body axis. Results of the study show that a direct phase measuring system operating at 8 GHz satisfies the accuracy requirements.

This interferometer system employs two primary receiving antennas separated by a distance of 34 inches (the base line) and located along a line which forms a space angle with a plane wavefront arriving from a distant radiating source. Ambiguity resolution is performed with an additional antenna pair at a 4.5 inch spacing. Thus, the arm of the subject interferometer is a 3-element collinear array.

A second array, having a base line orthogonal to the first, makes it possible to determine the angles made by the line-of-sight with a plane containing the two arrays. Since this arrangement cannot provide information regarding the rotation of that plane about the line-of-sight, two ground illuminators are employed.

The method of phase measurement chosen is one in which the RF signal is down-converted to a nominal 100 kc signal, whereby a small phase difference at the interferometer input is represented by a time increment that is measured by digital counting techniques. The time between zero crossings is employed to resolve the phase angle difference (count is proportional to phase difference). A scale factor converts this result into a signal which gives the direction of the RF wavefront relative to the baseline and the output of the scale factor circuit is fed to a geometrical transformation circuit which

converts phase difference into spatial attitude (pitch, roll, yaw). The pertinent features of the interferometer are:

- Type: Two axis, direct phase measuring
- Illuminating req.: 8 GHz (nominal)  
Stability:  $1:10^8$
- Number of Illuminators: 2
- Interferometer Configuration:
  - Baseline dimension: 34 inches
  - Number of arms: 2 orthogonal
  - Number of elements: 5
  - Element spacing: vernier: 34 inches  
(from reference element) coarse: 4.5 inches
- Sensor Accuracy  $\pm 0.014^\circ$  @ 30db SNR
- Attitude Determination Accuracy @ 30db SNR (including ephemeris errors):

| <u>Attitude</u>           | <u><math>0^\circ</math></u> | <u><math>\pm 10^\circ</math></u> | <u><math>\pm 30^\circ</math></u> |
|---------------------------|-----------------------------|----------------------------------|----------------------------------|
| Yaw axis error            | $\pm 0.09^\circ$            | $\pm 0.11^\circ$                 | $\pm 0.2^\circ$                  |
| Pitch and roll axis error | $\pm 0.005^\circ$           | $\pm 0.008^\circ$                | $\pm 0.02^\circ$                 |

#### 1.3.7 Phased Array

The phased array subsystem consists of a corporate fed planar array, located on the earth's side of the spacecraft. The antenna consists of a square arrangement of 64 high-gain hexagonal horns in a triangular matrix. (Figure 1.3-3). Highest gain with fewest elements and with minimum beam distortion in any direction of scan is achieved with the triangular spacing. The array dimensions are 31 inches by 36 inches. The minimum gain on the array axis is 32 db (including all system losses). The antenna beam which is circularly polarized will scan over a  $\pm 10^\circ$  coverage angle with less than a 3 db degradation at the edge. No grating lobes will fall within the earth's disk.



The half power beam width is approximately 2.2 degrees.

The complete system which includes two X-band transmitters and receivers, a simple beam steering unit, microwave system, and antenna, weighs less than 170 pounds. The ERP per pound is almost an order of magnitude greater than the Transdirective array. With the exception of the receivers, transmitters and beam steering unit, the system will be a passive one, capable of generating four beams which are steered independently by phasors, and which may be commanded by a single ground terminal. All modes of operation and test require a maximum data rate of 35 bits per second generated by the terminal computer. The four-beam array normally operates as a one-channel duplex system or a two-channel simplex system by adding a simple 192 bit memory bank to the beam steering unit. This causes the transmit and receive beam to interchange direction upon the reception of a coded signal. The coded signal is generated by the last terminal to transmit during a two-way conversation. The transfer may be made in a fraction of a second by a single bit tone.

The system can perform tracking for comparison with tracking error information generated by other systems on board. The attitude stabilization accuracies of  $\pm 0.1^\circ$  required for other subsystem functions aboard the spacecraft are an order of magnitude more precise than will be needed for the pointing of the array beam. The use of 3-bit digital phasors will permit better than an 0.2 beamwidth step scan interval resulting in precise beam pointing control and negligible scan loss.

The four channel microwave distribution system will consist of combinations of binary and series fed isolated dividers and combiners. The frequency of operation and the expected controlled temperature environment ( $40^\circ\text{F}$  excursion) combine to make the temperature compensated latching phase shifter ideally suited for this application. A strip line diplexing module

connects each of the 64-four channel sets of separate feed horns.

The study and analysis of four candidate systems has shown that the corporate fed array is the most reliable, efficient, high performance technique available for this application.

#### 1.3.8 In-Orbit Maneuvers and Auxiliary Propulsion System

The various in-orbit maneuvers which must be accomplished by the ATS-4 include correction of initial orbit injection errors, East-West and North-South station keeping, and East-West station repositioning. The guidance concept for executing all of these maneuvers is that the master ground station provides command-control based upon satellite track data. Thus, the ground station will decide when and how such maneuvers are to be made and command turn-on and turn-off for the proper thruster of the Auxiliary Propulsion System (APS).

Table 1.3-3 presents the velocity impulse requirements associated with these in-orbit maneuvers for the Auxiliary Propulsion System (APS). The predicted  $3\sigma$  synchronous orbit element errors for the SLV-3C/Centaur/Spin-Stabilized 364-3 were determined to be: period error of  $\pm 45$  min, eccentricity of 0.03 and inclination of  $\pm 1.08$  deg. The North-South station keeping velocity impulse is designed to compensate (for 1 year) the calculated orbit inclination buildup of  $0.75^\circ/\text{year}$  due to solar-lunar orbit perturbations. The East-West velocity impulse includes the 100 ft/sec specified for station repositioning and 20 ft/sec for 2 years of station keeping against earth gravitational perturbations. The latter figure includes a provision for compensating East-West velocity errors introduced by the North-South station keeping operations.

The most promising APS candidates were hypergolic bipropellant and hydrazine monopropellant propulsion systems. The latter is favored on the basis of reliability and development status, although the former has a slight weight advantage. Table 1.3-3 presents fuel and total weight

TABLE 1.3-3 ATS-4 AUXILIARY PROPULSION SYSTEM DATA

(Monopropellant Hyrazine:  $I_{sp} = 220$  sec.)

|                                          |        |
|------------------------------------------|--------|
| Velocity Requirements (ft/sec)           | 595    |
| Injection Errors ( $3\sigma$ , ft/sec)   |        |
| In-Plane                                 | 150    |
| Out-Plane                                | 195    |
| North-South Station Keeping              | 130    |
| East-West Station Keeping                | 120    |
| and Repositioning                        |        |
| Total Impulse (pound-seconds)            | 29,600 |
| (Based on maximum weight of 1605 pounds) |        |
| Fuel Weight (pounds)                     | 135    |
| Total APS Weight (pounds)                | 172    |

figures for the hydrazine monopropellant APS. A 1-pound thrust level is assumed for each of the 3 nozzles (2 East-West and 1 North-South) with an associated specific impulse of 220 seconds.

#### 1.3.9 Additional Experiment Capability

In addition to monopulse tracking and antenna pattern measurements capability, the ATS-4 communications systems provides various advanced relay services by reason of the large ATS-4 apertures. These services are:

- FM broadcast relay
- TV broadcast relay
- Teletype and voice links to aircraft
- Ground-to-ground voice links
- Geophysical data collection from low altitude satellites and unmanned ground stations.

The additional experiment capability will enable the ATS-4 satellite to provide high-quality communications to the public, industry, and government.

The frequencies chosen for these additional experiments are those that are already assigned to the service: FM at 100 MC, UHF TV at 800 MC, telemetered data at S-band and voice links at X-band. The broadcast relay experiments will demonstrate the feasibility of extending services to rural areas, at reasonable cost to the community, and with quality comparable to existing urban installations. The broadcast relay service will be especially useful to areas that are blocked from the mass communications media by terrain. With modest ground antennas and minimal equipment, the rural areas can receive the urban FM and TV programs without noticeable degradation. This is possible because of the high gain of the ATS-4 parabolic antenna.

A second category of additional services which are not now avail-

able includes:

- Long distance aircraft communications
- Gathering of geophysical data
- Direct line, high-capacity long-distance telephone links

These direct links are not constrained to particular centers that might already have overloaded trunk lines, but will be beamed to the most desirable central distribution point. Direct communications from global aircraft to home bases will have an immediate favorable impact on safety and traffic control and can eventually develop to airplane passenger telephone service from any part of the world.

There are large expanses on earth from which geophysical data is unavailable because of an hostile environment to man. Such areas can be "explored" with sensors attached to transmitters dropped in by aircraft. The data will then collected by the satellite, directly or through low altitude satellites, and relayed to a central ground station.

The long distance telephone, or teletype, link is feasible not only because of the gain of the phased array, but also because of the ease with which the high gain beam can be directed. Added to these features is the capability of having a number of beams functioning simultaneously and independently. This adds up to versatility, high capacity and high quality performance without restrictions of a single high-gain antenna beam.

All of the additional capability can be provided with 10-watt spacecraft transmitters. For the evaluation of the technical performance alone, 100-milliwatt spacecraft transmitters are sufficient. Thus, the ATS-4 system can provide these services with small additions to the basic equipment necessary to measure and evaluate its purely technical performance.

The larger transmitters weight an additional 21 pounds, compared to the minimum power transmitters, and require an additional 161 watts of primary power. The total spacecraft differential weight penalty, attributed

to the additional capability, is 75 pounds. Of the total, 54 pounds is associated with the larger power supply, and the remainder with the larger transmitters.